Optimize Your Research

Simple and Flexible Solution for Gas Analysis with HiCube RGA

Your added value

- Optimally integrated high-tech components with PrismaPro and an oil-free HiCube turbopumping station
- Can be used from atmospheric pressure to high vacuum
- High resolution and sensitivity
- Designed for universal use with digital and analog inputs
- Wide variety of applications for residual gas analysis, process monitoring, leak detection or quality control of vacuum processes

Pfeiffer Vacuum GmbH
Germany
T +49 6441 802-0

PFEIFFER VACUUM

Your Success. Our Passion.

www.pfeiffer-vacuum.com

Guest Editor: Mats Larsson

ACCELERATOR MASS SPECTROMETRY

Ragnar Hellborg* and Göran Skog

Department of Physics, Lund University, Sölvegatan 14, SE-223 62 LUND, Sweden
[2]GeoBiosphere Science Centre, Quaternary Sciences, Lund University, Sölvegatan 12, SE-223 62 Lund, Sweden

Received 19 April 2007; accepted 16 October 2007

Published online 9 May 2008 in Wiley InterScience (www.interscience.wiley.com) DOI 10.1002/mas.20172

In this overview the technique of accelerator mass spectrometry (AMS) and its use are described. AMS is a highly sensitive method of counting atoms. It is used to detect very low concentrations of natural isotopic abundances (typically in the range between 10^{-12} and 10^{-16}) of both radionuclides and stable nuclides. The main advantages of AMS compared to conventional radiometric methods are the use of smaller samples (mg and even sub-mg size) and shorter measuring times (less than 1 hr). The equipment used for AMS is almost exclusively based on the electrostatic tandem accelerator, although some of the newest systems are based on a slightly different principle. Dedicated accelerators as well as older "nuclear physics machines" can be found in the 80 or so AMS laboratories in existence today. The most widely used isotope studied with AMS is ^{14}C. Besides radiocarbon dating this isotope is used in climate studies, biomedicine applications and many other fields. More than 100,000 ^{14}C samples are measured per year. Other isotopes studied include ^{10}Be, ^{26}Al, ^{36}Cl, ^{41}Ca, ^{59}Ni, ^{129}I, U, and Pu. Although these measurements are important, the number of samples of these other isotopes measured each year is estimated to be less than 10% of the number of ^{14}C samples. © 2008 Wiley Periodicals, Inc., Mass Spec Rev 27:398–427, 2008

Keywords: *accelerator mass spectrometry (AMS); radioisotopes; isotopic composition; tandem accelerator; cosmogenic isotopes*

I. INTRODUCTION

There is a need to detect very low concentrations of atoms in a sample in a number of research fields and technical applications. Several nuclear physics techniques have been developed, some of them with depth resolution and sensitivity that cannot be achieved with any other technique, either physical or chemical. In a particle accelerator, beams of fast, ionized atoms are produced. The type of ion, ion energy, intensity, and geometrical dimensions of the beam can often be chosen rather freely. This has made it possible to develop a number of analytical techniques with extremely high resolution and sensitivity. Some of these techniques and their qualities are listed in Table 1. For a detailed description of most of these techniques, see for example Brune et al. (1997).

One of the applications of nuclear physics techniques that is listed in Table 1, and which has been of great benefit to other fields of scientific endeavor, is accelerator mass spectrometry (AMS). The capability of AMS in extremely sensitive radioisotope measurements has been extensively demonstrated over the past 30 years. For example, AMS has allowed refinements in the technique of ^{14}C dating in the fields of archeology and quaternary geology. The most important improvement compared to traditional radiometric methods is the possibility to date small samples with AMS. Using AMS the radiocarbon age of a 10,000-year-old sample of 1 mg or less can be determined with a precision of ±40 years in less than 30 min. To achieve the same precision with radiometric methods the sample must contain more than 1 g of carbon and counting must proceed for over 24 hr.

As the number of AMS facilities has grown, the number of applications has increased. ^{14}C is still the most important AMS isotope, but other applications, apart from traditional dating, are directed towards studies of atmospheric processes and ocean circulation to gain information about past climates. ^{14}C-AMS has also found applications in biomedical studies. Other isotopes such as ^{10}Be and ^{36}Cl have been used to gain hydrogeological information. These two isotopes are also trapped in the ice sheets of Greenland and Antarctica, where they can be used as tracers of the solar and geomagnetic modulation of the cosmic radiation reaching the earth. Cosmic ray exposure also causes the build-up of ^{10}Be, ^{26}Al, and ^{36}Cl in surface rocks. The accumulated amounts of these isotopes can be measured by AMS and used to date the rock (so-called exposure dating). ^{26}Al-AMS has also been used to study metabolic processes in living systems. The production of ^{41}Ca from nuclear weapons testing has been measured by AMS, and ^{36}Cl and ^{129}I have been used to trace the migration of nuclear waste from nuclear storage and reprocessing plants and nuclear power plants.

Although various types of accelerators can be used, almost all AMS systems employ the electrostatic tandem accelerator. Rare isotopes from a sample material placed in the ion source of the tandem accelerator are measured by counting individual atoms with nuclear detection techniques after acceleration up to

**Correspondence to:* Ragnar Hellborg, Department of Physics, Lund University, Sölvegatan 14, SE-223 62 LUND, Sweden.
E-mail: ragnar.hellborg@nuclear.lu.se

TABLE 1. Different analytical methods using beams of fast ions and neutrons

Method[1]	Information Depth / μm	Resolution Depth // Lateral	Sensitivity[2]	Sample	Facilities worldwide // cost / Eur
RBS	2	25 nm // 0.5 mm	10^{-4}–10^{-7}	Solid / 0.25 mm^2	500 // 70
ERDA	1	20 nm // 1 mm	10^{-4}–10^{-5}	Solid / 5 mm^2 [3)]	300 // 100
NRRA	2	10 nm // 1 mm	10^{-5}	Solid	300 // 200
NRA	0.1–1	5–10 nm // 1 mm	10^{-4}–10^{-7}	Solid / 3 mm	300 // 200
PIXE	50	10 μm // 1 μm	10^{-6}–10^{-7}	Solid/powder / 1 mm	300 // 50
CPAA	100	– // 1 mm	10^{-7}–10^{-8}	Solid / 1mm^2	100 // 1000
AMS			10^{-14}-10^{-15}		100 // 400

[1] RBS, Rutherford backscattering; ERDA, elastic recoil detection analysis; NRRA, nuclear resonance reaction analysis; NRA, nuclear reaction analysis; PIXE, particle induced X-ray analysis; CPAA, charged particle activation analysis; AMS, accelerator mass spectrometry.
[2]Number of atoms per number of host atoms.
[3]Glancing incidence beam—and glancing exit beam.

energies in the range of 0.2–40 MeV (a few very large tandem accelerators produce even higher energy beams). Compared to conventional mass spectrometry, the dramatic improvement in background rejection in the AMS systems has, in some cases, led to a 10^8 times increase in the sensitivity of isotope ratio measurements.

Accelerator mass spectrometry (AMS) evolved at nuclear physics laboratories where tandem accelerators were originally installed during the 1960s and 1970s. Most of these cannot produce beams with sufficient energy for today's nuclear physics experiments, and were therefore adapted for AMS due to the need to date small samples of ^{14}C. During the late 1970s a great deal of effort was devoted to the evaluation of tandem accelerators for AMS detection of ^{14}C. One important discovery was that ^{14}N does not form stable negative ions (Purser et al., 1977). It was then soon shown that ^{14}C can be detected at the very low, natural isotope ratio of $^{14}C/^{12}C = 10^{-12}$ (Bennett et al., 1977; Nelson, Korteling, & Stott, 1977). The first dedicated AMS systems were installed in the early 1980s (Purser, Liebert, & Russo, 1980). During the past decade (up to 2007), the best achievements have been obtained with relatively small accelerators designed for and dedicated to AMS measurements.

Accelerator mass spectrometry (AMS) is an expensive technique and it is also technically complicated. Therefore, the most significant technical development during the past 10 years is the trend towards smaller AMS systems. The reduction in floor space and overall cost are the most attractive features of these new systems, as well as the smaller technical staff required to run the systems.

The development of AMS has been reviewed in many articles, one of the most recent being that by Kutschera (2005). Every third year an international conference on AMS is organized. The most recent one was held in Berkeley California, USA in September 2005 (The 10th International Conference on Accelerator Mass Spectrometry, Nucl Instrum Methods B, in press). The next one will take place in Rome, Italy in September 2008.

The instrumentation and general principles of AMS will be discussed in Section II. Some recent technical developments, such as the trend towards smaller accelerators and attempts with other types of accelerators, will be described in Section III. Some examples of the application of AMS are presented in Section IV. Finally, in Section V conclusions and future perspectives are discussed.

II. GENERAL PRINCIPLES AND INSTRUMENTATION

A. Principles of AMS

The two standard methods used for a long time to determine the isotopic composition of an element are mass spectrometry (MS) and decay counting. While MS can be used for all isotopes, decay counting is restricted to radioisotopes. For long-lived radioisotopes decay counting is inefficient because only a small fraction of the nuclides in a sample decays during a reasonable measurement time. Conventional MS has a high efficiency but it is limited to isotope ratios greater than approximately 10^{-7}. In

AMS the efficiency of MS is combined with extremely good discrimination against isobaric, isotopic, and molecular interference. In Figure 1, the efficiency of decay counting and AMS are shown as a function of half-life ($T_{1/2}$). The efficiency is defined as the number of atoms detected compared to the number in the sample. The counting time for AMS is assumed to be 1 hr, while the efficiency for decay counting periods of 24 hr and 14 days are shown in the figure. The high discrimination of AMS is obtained by accelerating the ions to a high energy, usually employing an electrostatic tandem accelerator. For a detailed description of electrostatic accelerators see for example Hellborg (2005). In a few cases other types of accelerators are used, this is further outlined in Sections IIIA and IIIB. A typical AMS system includes the following:

1. Production of negative ions in a multi-sample, negative-ion source. The sample material containing the rare isotopes to be counted is placed in the ion source.
2. Acceleration of negative ions from ground potential to a high positive voltage.
3. Recharging of all ions to positive by stripping off electrons and at the same time dissociation of all molecular ions.
4. Acceleration of the now positive ions back to ground potential (exception, see Section IIIA).
5. The removal of unwanted ions using electric and magnetic fields.
6. Identification and counting of the individual rare isotopes with nuclear detection techniques.
7. Computer control of the accelerator system to allow for unattended operation and to provide control of the AMS system parameters.

Accelerator mass spectrometry (AMS) is an extension of MS including an accelerator. In Figure 2 an MS system is compared with a simple AMS system. The introduction of the tandem accelerator, followed by several ion-filtering devices reduces the background by a factor of the order of 10^8. Three especially important characteristics of AMS allow the measurement of low isotope ratios (for example, for $^{14}C/^{12}C$ down to 10^{-15}).

i. Interference by some isobars is avoided by using a negative ion source (for example, $^{14}N^-$, $^{26}Mg^-$, $^{55}Mn^-$, and $^{129}Xe^-$, all with negative electron affinity, when detecting ^{14}C, ^{26}Al, ^{55}Fe, and ^{129}I).
ii. Interference by molecules is avoided by using a stripper system in the high-voltage terminal of the accelerator (for example, $^{12}CH_2$ and ^{13}CH when detecting ^{14}C). In the stripping process the negative ions become positive, and at the same time, nearly all the molecular ions will be dissociated. A few molecular ions with a maximum charge state of 2+ will survive. Molecular ions can thus be avoided by choosing a charge state higher than 2+ with the high-energy analyzing system after the accelerator.
iii. The counting of individual ions is possible due to their high final energy. The ions that reach the detector are easily separated by their energy difference.

To demonstrate some technical details of an AMS system, we will take a closer look at the AMS system at the Pelletron in Lund, shown in Figure 3. A beam of negative ions is formed in the ion source (a), and the beam is analyzed by an electrostatic (e) and a magnetic (f) analyzer in the injector. The electrostatic analyzer bends the beam to make it vertical while the magnetic analyzer bends the beam back to the horizontal. The ion source is thus elevated relative to the accelerator. Optical devices (einzel lenses/quadrupole lenses) are placed at several positions

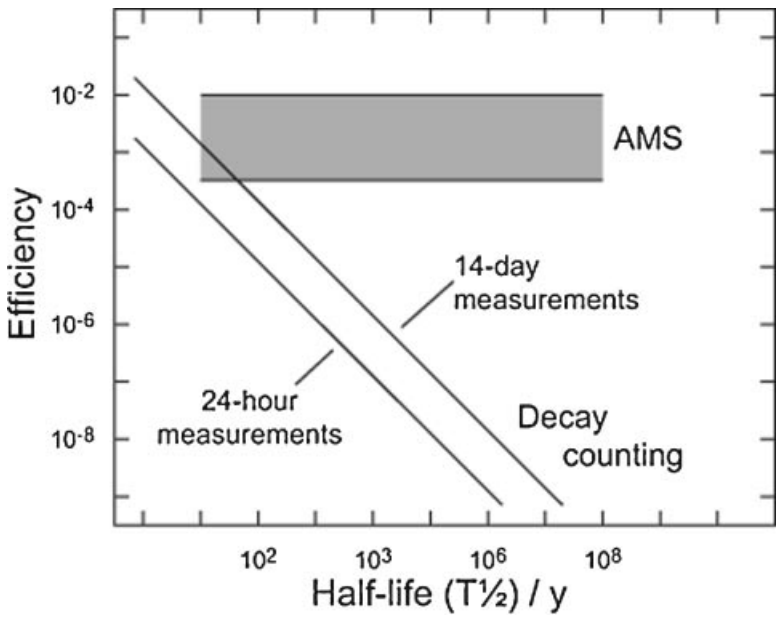

FIGURE 1. The efficiencies of AMS and decay counting as a function of half-life. For details, see the text.

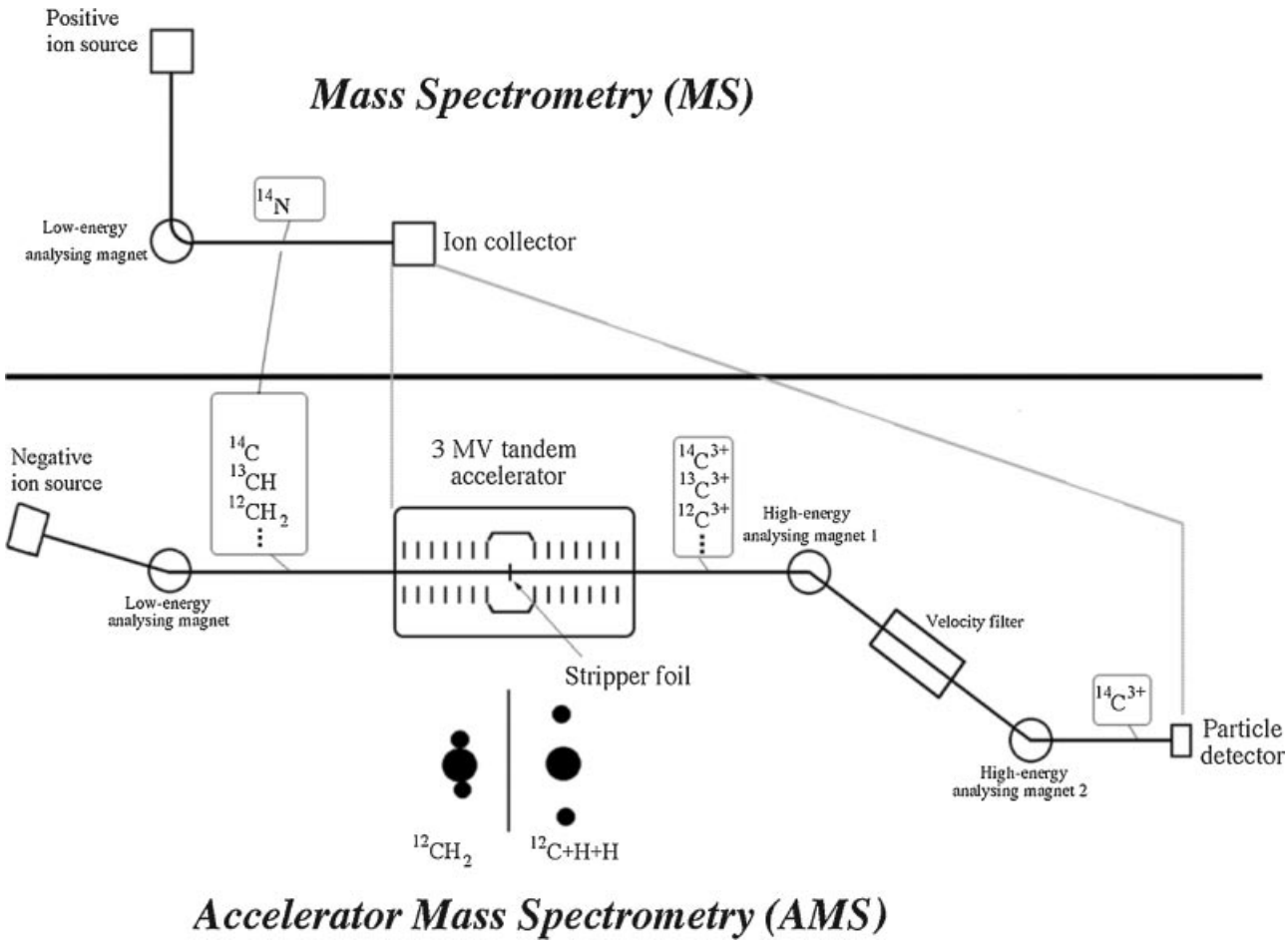

FIGURE 2. Comparison between MS and a typical AMS system.

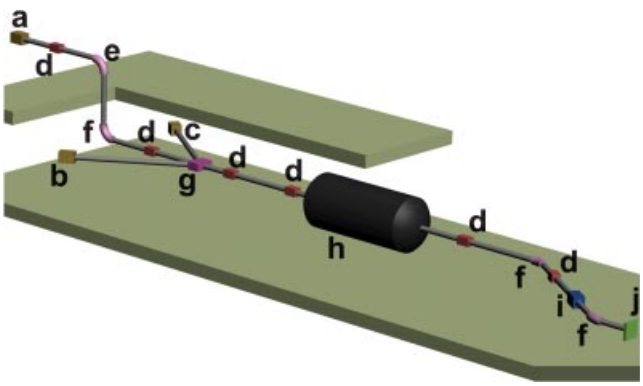

FIGURE 3. An outline of the AMS system at the Pelletron in Lund (in use for AMS from 1988 to 2005). **a**: Second-generation AMS source (of the type shown in Fig. 4); **b**: off-axis duoplasmatron source for purposes other than AMS; **c**: first-generation AMS source (of the Cs-gun type); **d**: einzel/quadrupole lens; **e**: spherical electrostatic analyzer; **f**: magnetic analyzer; **g**: magnetic analyzer with three entrance ports; **h**: electrostatic tandem accelerator; **i**: velocity selector; **j**: particle detector. [Color figure can be viewed in the online issue, which is available at www.interscience.wiley.com.]

along the beam line to keep the beam envelope as small as possible (d). The beam of negative ions is transported to the accelerator and accelerated to the positive high-voltage terminal of the tandem accelerator (h). In the high-voltage terminal, the negative ions pass through a foil or a gas cell. The negative ions, now at a high energy, will lose electrons and become positively charged. Molecular ions are dissociated in the foil or gas and can therefore not interfere. The positive ions are accelerated to ground potential through the second stage of the accelerator and gain a further increase in energy. The beam of positive ions is analyzed by a magnetic analyzer (f) and the ions of interest are selected. The beam is further analyzed by a velocity selector (i) and once more by a magnetic analyzer (f).

The selected ions will have well-defined charge state, energy, and mass. They are identified and counted one by one using a detector (j). The ions are identified by their energy. This is necessary as ions other than those desired can reach the detector. The various components of the AMS system are described in more detail in Section IIB.

As mentioned above, decay counting and conventional MS both have certain fundamental limitations compared to AMS,

especially for rare, long-lived radioisotopes. We will illustrate these limitations with the following example for ^{14}C: 1 g of modern carbon contains 6×10^{10} atoms of ^{14}C (the number of ^{12}C atoms is 1.2×10^{12} times more). Only around 13 of these ^{14}C atoms will decay per minute. To obtain a statistical precision of 0.5% (which is often required in radiocarbon dating) using 1 g of carbon, it is necessary to count the decays for more than 48 hr. When using mass spectrometer techniques it is not necessary to wait for the atoms to decay, and this alternative is therefore, in principle, much more efficient. However, conventional MS cannot be used as the ^{14}C ions are masked by an intense flux of the atomic isobar ^{14}N and by molecular isobars with the same mass, such as ^{13}CH, $^{12}CH_2$, ^{12}CD, and $^{7}Li_2$. Also, the ''tails'' of the stable isotopes ^{12}C and ^{13}C contribute to the background in MS. These factors mean that MS can only be used for isotope ratios of $^{14}C/^{12}C$ of approximately 10^{-7} or higher. By employing AMS instead, the $^{14}C/^{12}C$ detection limit can lowered to approximately 10^{-15}. For AMS, a sample of 1 mg carbon is sufficient, that is, only one thousandth of the material needed for decay counting. A 1 mg sample will be completely sputtered in the ion source within an hour or two and typically 6×10^5 atoms can be counted in the AMS detector, which is 1% of the total ^{14}C content.

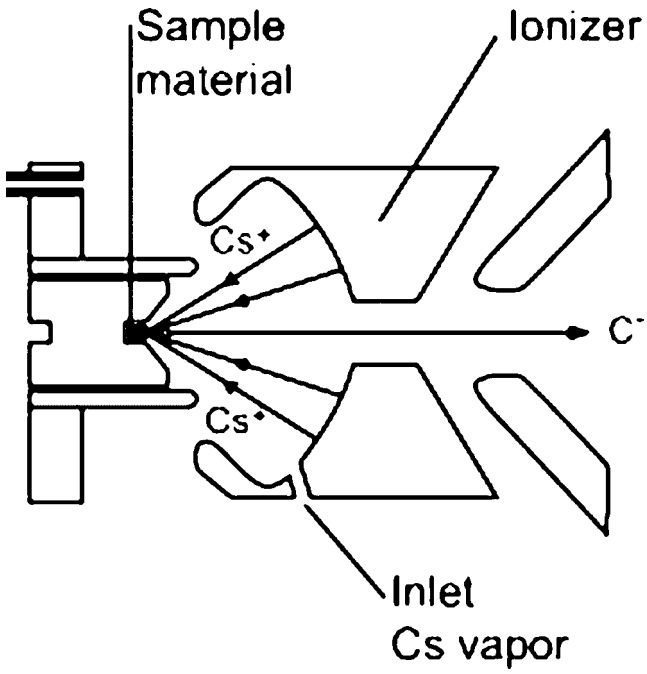

FIGURE 4. The geometry of a Cs sputter ion source.

B. Traditional AMS Instrumentation

1. The Ion Source

In a tandem accelerator, negatively charged ions gain energy by attraction to the high positive voltage at the geometric center of a pressure vessel. Thus, a negative ion source is needed. The requirements on such a source designed for AMS are a high, stable ion beam current and a high efficiency for negative ions. The source should also be equipped with a multiple sample holder for fast switching between different samples. The cross-contamination or ''memory effect'' between successive samples should be negligible. A source working with solid samples, fulfilling these requirements, is the cesium negative ion source, which was introduced around 1970 (Middleton & Adams, 1974). The principle of such a source is that cesium ions of a few keV are focused on the surface of a solid sample and enough energy is transferred to the target material to produce free atoms and ions of the sample material. This process is called sputtering. In the original versions positive Cs ions were created by an oven and a surface ionizer placed some distance away from the sample. The Cs^+ ions were then extracted by an acceleration gap and a Cs^+ beam is focused onto the sample by a lens system. This is often referred to as a cesium gun source, and it is still in use at a few laboratories. Today, cesium sputter sources with a hot tantalum ionizer and the sample in the same volume are more common, see Figure 4. Cesium vapor from an oven hits the ionizer, the Cs atoms are ionized and the positive Cs^+ ions are accelerated and focused on the sample, which is maintained at a negative potential compared to the ionizer, and atoms are sputtered from the sample. Neutral atoms, as well as positive and negative ions, will be sputtered from the sample surface. As the sample is at a negative potential, negatively charged ions are accelerated away from the sample and a beam of negative ions is obtained, which is extracted through an aperture. Certain amounts of the Cs vapor will condense on the sample and produce a thin surface layer. The advantage of Cs (and some other group IA elements) over other heavy elements, which could also be used for sputtering, is that this surface layer will considerably reduce the work function (the energy difference between a free atom and an atom bound at the sample surface).

A charged particle beam is specified by its energy and its emittance. The emittance is defined as the ''volume'' in the four-dimensional phase space (x,y,v_x,v_y) that is occupied by the ion beam. x and y are positions in two orthogonal transverse directions, and v_x and v_y are the corresponding velocity components. The emittance of the beam leaving the ion source is partly determined by the processes occurring in the ion source and partly by the design of the source. A low numerical value of the emittance is desirable as it means low transverse dimensions of the beam after it has passed some distance along a drift section.

The ionization efficiency, that is, the fraction of the atoms sputtered from the sample which becomes negative and has an emittance that can be transmitted through the accelerator compared to the total number of sputtered atoms, is 1–2% for a Cs source. A few examples of the type of sample material used for different isotopes, the type of ions produced, the corresponding stable isotope and typical beam currents for the stable isotope are given in Table 2.

A sputtering source fed with a gaseous CO_2 sample, as an alternative to solid graphite samples, was introduced at the AMS laboratory in Oxford, UK a number of years ago (Bronk Ramsey & Hedges, 1990). Today, a number of AMS laboratories have reported the use of sputtering sources using CO_2 (see reports in The Proceedings of the 10th International Conference on Accelerator Mass Spectrometry, Berkeley, CA, USA, Nucl Instrum Methods B, in press). The advantage of using gaseous

TABLE 2. Sample material, rare and stable isotopes and current of stable isotopes for a few isotopes used in AMS

Isotope	Sample material	Rare ion	Stable ion	Current of stable ion /μA
^{10}Be	BeO	$^{10}Be^{16}O^-$	$^{9}Be^{16}O^-$	5–10
^{14}C	Graphite	$^{14}C^-$	$^{12}C^-$, $^{13}C^-$	30–100
^{26}Al	Al_2O_3	$^{26}AlO^-$	$^{27}AlO^-$	1–5
	Al_2O_3	$^{26}Al^-$	$^{27}Al^-$	0.1–1
^{36}Cl	AgCl	$^{36}Cl^-$	$^{35}Cl^-$	10–20
^{59}Ni	Ni	$^{59}Ni^-$	$^{58}Ni^-$	1–5

carbon samples is twofold. A much simpler sample preparation procedure (see Section IIB.6) can be used, as the second step of reducing the gas to solid carbon is unnecessary, and very small samples can be analyzed. (Samples down to 1 μg have recently been reported to have been analyzed (Uhl et al., 2007).) The disadvantage of gaseous material is a lower beam current and a higher risk of cross-contamination between different samples.

2. *The Injector and Low-Energy Analyzing System*

The low-energy (∼5–10 keV), diverging beam leaving the ion source is accelerated, focused and transported to the entrance of the accelerator by the injector system, see Figure 3. This system consists of a short accelerating gap, apertures that define the emittance of the beam, lenses, and steerers, beam stops to measure the beam current, and other diagnostic equipment used to obtain information about the beam. The pre-acceleration voltage, just after the source, is in the range of 30–300 kV. The higher the beam energy, the better the beam's optical fit to the entrance of the accelerator. The purpose of the injector is to function as a traditional mass spectrometer to ensure that only ions of the correct mass are injected into the accelerator. To achieve this, one or more magnetic analyzers are always part of the injector. One disadvantage of the Cs sputter ion source is that the ion beam produced has a high-energy tail. Thus, when high mass and energy resolution is required (as is the case with ^{36}Cl-AMS) an electrostatic analyzer (see Fig. 3) must be included. To obtain the same focusing conditions for all isotopes, all the lenses and steerers in the injector system should be electrostatic so as to be mass independent. Two different types of specialized injector systems have been developed for AMS: "sequential" and "simultaneous" injection.

Most systems use sequential injection. The switching between the stable and the rare isotope, which is necessary for normalization purposes, is achieved by applying different voltages to the electrically insulated vacuum chamber of the analyzing magnet. When entering and leaving the magnet chamber the ions will be accelerated and retarded, respectively. In this way, the two different isotopes have different energies when passing the magnetic field, which is kept constant. The alternative, that is, switching between different magnetic fields, is much slower and therefore not practical. The numbers of ions of the stable and rare isotopes produced in the ion source per unit time are several orders of magnitude different compared to each other. Therefore, the electrical load on the accelerator tube will be very different and, as a result, the high voltage of the tandem can vary. To minimize this effect the stable isotopes should be injected with a much shorter time period than the rare isotope. Typical repetition rates are 10 sec^{-1}. Over 90% of the time is used to inject the rare isotope. The beams of the stable isotopes are injected into the accelerator as short pulses, typically 100 μsec long, in order to avoid beam loading. The injector shown in Figure 3, with the vertically mounted analyzing magnet, has a vacuum chamber insulated from ground potential and is thus of the sequential type.

An alternative to sequential injection is simultaneous injection (Purser, Smick, & Purser, 1990), which is used for ^{14}C-AMS in some laboratories. In this case, the stable and rare

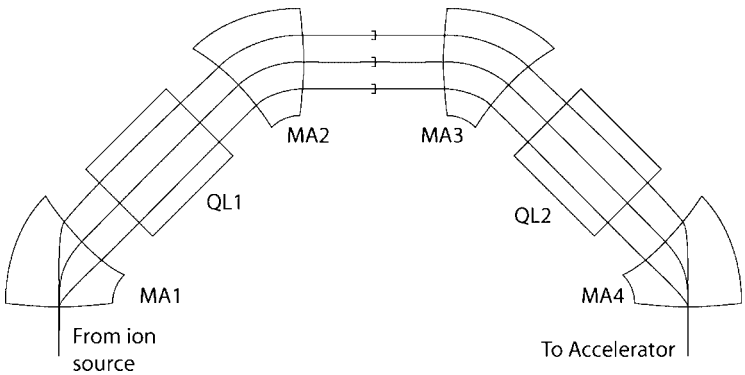

FIGURE 5. A simple illustration of a "simultaneous" injector. QL = quadrupole lens, MA = magnetic analyzer. The paths shown for three isotopes are only schematic and not "beam optically" correct.

isotopes are injected into the accelerator together. This is achieved by a sequence of magnetic analyzers and quadrupole lenses allowing the different isotopes to follow different trajectories after leaving the source. Finally, they are recombined before entering the accelerator. A very simple sketch of a simultaneous injector is shown in Figure 5. At the mirror plane of the arrangement the three beams of mass 12, 13, and 14 are parallel and separated by ~20 mm. A rotating, slotted wheel (not shown in the figure) is positioned in the mass 12 path close to the mirror plane, where the separation of the isotope paths is at a maximum Only ~1% of the ^{12}C ions pass through this wheel, thus avoiding a current load on the terminal.

3. The Tandem Accelerator

The electrostatic accelerator, first demonstrated at the beginning of the accelerator era more than 75 years ago, is the accelerator type with the greatest energy stability. The high voltage in an electrostatic accelerator is created by a mechanical transport system, which continuously transports charges from ground to the insulated high-voltage terminal. All tandem accelerators with a maximum terminal voltage above 5 MV use such a mechanical system. For tandem accelerators up to 5 MV either a mechanical transport system (i.e., an electrostatic accelerator) or a multiplying rectifier-condenser system (a cascade accelerator) is used. For technical details about different principles of accelerator design, see Hellborg (2005). The open air accelerator fails above a few MV, mainly because of the moisture and dust in the air, which generate sparks. For this reason, and also to reduce the physical dimensions, the whole accelerator is enclosed in a tank containing a gas of high electrical strength, for example SF_6, at a high pressure (normally 0.6–0.7 MPa).

Tandem accelerators with very different maximum design voltages are today used for AMS. The very small machines with voltages below 1 MV (for further details see Section IIIA) became available in around 2000, after a very successful demonstration by the AMS group in Zurich, Switzerland (Suter, Jacob, & Synal, 1997). It was mainly developed for radiocarbon AMS, but promising results for ^{10}Be, ^{26}Al, ^{41}Ca, ^{129}I, and Pu have also been reported. Accelerators with terminal voltages between 1 and 3 MV have been installed at a number of laboratories, mainly as dedicated AMS facilities. They are predominately used for ^{14}C measurements, but ^{10}Be, ^{26}Al, and ^{129}I are also measured. In the 3–10 MV range a number of older, nuclear physics machines from the 1960s and 1970s have been used for AMS, but there are still a few new accelerators up to 5 MV that are dedicated mainly to AMS. With a few exceptions, all isotopes measured in AMS are covered by these accelerators. (For example, the quantification of ^{59}Ni at natural levels requires a very large accelerator.) A few nuclear physics accelerators with voltages above 10 MV are used for AMS, mainly for development work for new isotopes. Approximately 10–20% of the operational time of these large accelerators is devoted to the development of AMS.

An important parameter for an AMS system is the transmission of ions from the ion source to the detector. It should be high and reproducible, and it should be insensitive to small changes in the injector or accelerator parameters. A high, flat-topped transmission through different optical elements is obtained with a well designed ion optical system, using large-diameter tubes, vacuum chambers and apertures. In the high-voltage terminal the negative ion beam is recharged or "stripped," that is, two or more electrons are removed from each ion. After stripping the ions are positive and are thus accelerated back to ground potential in the high-energy part of the accelerator. Stripping is performed by passing the beam through a thin foil or a gaseous medium. The advantage of a gas stripper compared to a foil stripper is better beam transmission stability through the accelerator over time. Due to radiation damage and thickening of the foil, the transmission through a foil will change with time. The disadvantages of gas stripping are a lower beam transmission and a lower mean charge state of the positive beam at a given high voltage. For light ions foil stripping can be used, for heavy ions gas stripping is necessary as the lifetime of the foils is too short for heavy ions. In all modern tandem accelerators, gas stripping is used, and it is combined with terminal pumping. With this equipment the stripper gas leaking out of the stripper chamber is re-circulated back to the stripper chamber instead of diffusing out through the accelerator tubes. In this way, a higher gas pressure can be used in the stripper chamber and a lower gas pressure (and therefore better vacuum conditions) can be maintained in the accelerator tubes. At higher pressure in the tubes, the transmission decreases as the beam is spread by collisions and by charge-exchange processes.

4. The High-Energy Analyzing System

A lens is needed close to the high-energy side of the accelerator to focus the diverging beam leaving the accelerator. Most AMS systems operate with beam energies of 10 MeV or higher. In this energy range only magnetic lenses are realistic. If an electrostatic lens were to be used it would have to be designed for several hundred kV, which in practice is impossible. The focused beam will enter a magnetic dipole—the analyzing magnet—in which the combination of mass, energy and charge, expressed as mE/q^2, will be selected. The stable isotopes can be collected at off-axis beam stops in the focal plane of the magnet. After a second focusing lens, additional analyzing equipment, such as an electrostatic analyzer (sorting after E/q) or a velocity selector (an electric and magnetic field perpendicular to each other and the beam direction, sorting after E/m) should follow. The purpose of this equipment is to remove the unwanted ions and molecular fragments that pass through the analyzing magnet with the correct value of mE/q^2. Without "cleaning up" the beam in this way, the background in the detector will be too high.

The number of unwanted ions passing through the analyzing magnet depends strongly on the pressure in the high-energy acceleration tube. At higher pressure (around 10^{-3} Pa or higher) more ions will change charge state during their passage through the high-energy tube, and some of them will fulfill the selected mE/q^2 value of the analyzing magnet. To obtain as low a pressure as possible in the high-energy tube, the gas stripper should, as was pointed out above, be supplied with pumps on both sides of the high-voltage terminal to re-circulate the stripper gas. Furthermore, pumps with high pumping speed should be placed as close as possible to the accelerator on both sides of the accelerator tank.

5. Detectors

A number of different types of detectors, originally developed for nuclear physics research, are used to count the rare isotopes in AMS experiments. The most common types of detectors are briefly described below.

a. Gas ionization detectors. This type of detector consists of a chamber filled with a suitable gas. The ions enter the gas chamber through a thin window, usually 1–2 μm Mylar. The ions will lose some energy and the ion beam will have a broader energy distribution after passing through the window. The most commonly used ionization gas is propane, but isobutene and a mixture of 90% argon and 10% methane are also used. When the energetic ions travel through the gas, free electrons are produced during the slowing down process. An electric field orthogonal to the beam direction causes the electrons to drift towards an anode. If the anode is divided into several parts, these different parts collect those electrons produced just beneath it. In this way the energy loss of the ions along that part of its track can be measured. Ions with different Z, that is, nuclear charge, lose energy at different rates (dE/dx). This type of detector can therefore measure not only the total energy of the ion but also its rate of energy loss as it slows down in the gas. With this detector, isobars such as ^{36}Cl and ^{36}S having identical total energy, can be separated. This type of detector is very robust and has a nearly infinite lifetime. The gas flows continuously through the chamber and only the entrance foil has to be replaced after a certain period of use. At some laboratories, a surface barrier detector (see below) is placed at the end of the chamber to measure the residual energy.

b. Surface barrier detectors. This type of detector, also called semiconductor detectors, is based on crystalline semiconductor materials, usually silicon and germanium. The basic operating principle is analogous to ionization devices, but the medium is a solid material. The surface barrier detector only measures the total energy of the ion, but has a better energy resolution than the gas ionization detector. In many cases where the background ions have a different energy from the rare ions this is sufficient for unique identification of the rare isotope. The sensitivity of this detector to radiation limits its lifetime. The energy resolution decreases as a function of the total dose. If the very intense beam of the stable isotope accidentally hits the silicon detector, it will be destroyed in a fraction of a second.

c. Time-of-flight detectors. The energy resolution of the gas ionization detector and the surface barrier detector deteriorate with increasing ion mass. For heavy ions, where neighboring masses can no longer be resolved these types of detectors have to be combined with a time-of-flight system (TOF) to obtain better resolution.

A TOF system consists of a ''start'' detector and a ''stop'' detector. The distance along the ion pathway between the two detectors is often a few meters. The start detector could be a thin carbon foil (today diamond-like carbon foils with a thickness as low as 0.5 μg/cm^2 and with very long lifetime are available (Steier et al., 2005)). The ions will pass through the foil with very limited energy loss. When the ions pass through the foil, electrons are emitted from the foil. These electrons are collected and multiplied by a micro-channel plate to obtain an electrical pulse. The stop detector can also be a thin foil followed by a silicon detector or an ionization chamber. An alternative to the stop foil is to use a silicon detector for both the stop signal and for energy detection. By measuring the time between the two signals, the speed of the ion is obtained. Time resolution down to 300–500 psec can be obtained. With this information, together with the total energy of the ion, ions such as ^{129}I and ^{127}I can be separated. This is impossible using only a gas ionization detector or a silicon detector.

d. Gas-filled magnets. During the 1950s nuclear physicists found that isobars (i.e., particles with the same mass) with the same energy traveling through a gas-filled region (pressure of 100–1,000 Pa) within a magnetic field orthogonal to the ion pathway followed different trajectories within the magnetic field. As isobars have different Z their average charge states are different in the gas zone. Therefore, they will also have different radii of curvature as long as they are within the magnetic field. An ionization chamber, placed at an appropriate bending angle after the gas zone and the magnetic field, will collect the rare isotopes. All other isotopes having other radii of curvature will miss the detector. A review of gas-filled magnets for AMS can be found in Paul (1990).

e. X-ray detectors. In the middle of the 1990s an alternative technique to TOF was demonstrated, which makes it possible to detect heavier isotopes, even with a small accelerator. The innovation in this technique is that, instead of detecting the ions directly, they are slowed down in a suitable target and the characteristic X-rays produced in this process are counted with an X-ray detector. In this way interfering isobars are suppressed. When a fast ion travels through a material it will interact with the atoms in the material, and the ions and the atoms in the material will be excited. Their de-excitation leads to the emission of X-rays characteristic of the atomic numbers of the atoms in the material and of the impinging ions. The detection of characteristic X-rays from atoms in a material was first demonstrated at the end of the 1960s to be a means of identifying tiny amounts of atoms in a substrate (Johansson, Akselsson, & Johansson, 1970). The method is called particle induced X-ray emission (PIXE) and has today developed into an important analytical tool (Johansson, Campbell, & Malmqvist, 1995).

The X-ray production depends strongly on the combination of the atomic numbers of the projectile ion and the target atom, due to the formation of molecular orbits. The X-ray yield from the target atoms decreases strongly as the atomic number of the target material increases. The X-ray yield from the projectile ions has a maximum for a target atomic number slightly above that of the projectile. Figure 6, from an investigation of nickel ions in Lund (Wiebert et al., 1996) demonstrates the X-ray yield as a function of the target atomic number. As can be seen from the figure, to achieve the highest detection efficiency a Cu or Zn target should be used in the case of a Ni beam. The X-ray yield for a Ni beam and different target materials has also been measured as a function of the beam energy. From Figure 7 it is evident that the X-ray yield increases with projectile energy.

The X-rays are detected by a high-resolution germanium or silicon detector (resolution 145 eV full width at half maximum (FWHM) at an X-ray energy of 5.9 keV). By measuring the characteristic X-rays emitted by the ions isobar separation can be obtained at ion energies where ionization chambers and surface barrier detectors give too poor discrimination. (For example, the

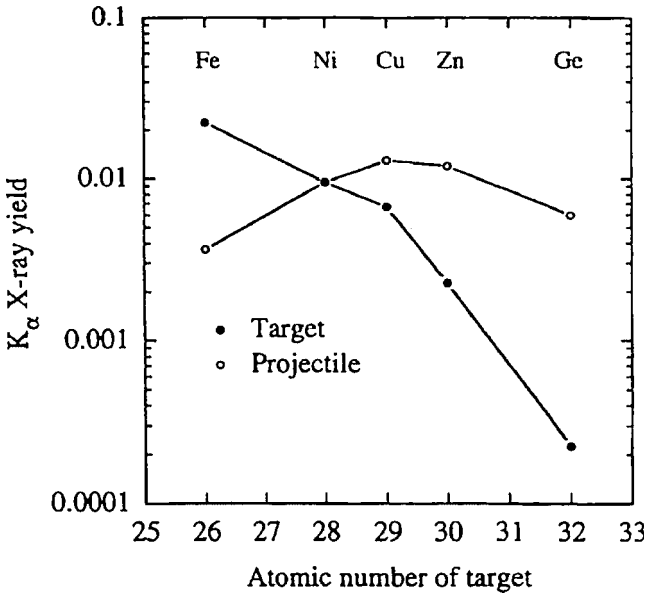

FIGURE 6. The total number of projectile and target K_α X-ray photons produced per ^{58}Ni projectile as a function of the atomic number of the target. Projectile energy 22 MeV. Lines are drawn only to guide the eye. (Reprinted from Wiebert et al. (1996), copyright 1996, with permission from Elsevier.)

energy difference between the K_α X-rays of the rare nuclide ^{59}Ni and its stable isobar ^{59}Co is ~700 eV.) Using a detector with an area of a few hundred mm^2 placed close to the vacuum chamber only about one X-ray quantum is detected per incoming 10^4 ions. Despite this fact, the technique of measuring characteristic X-rays in AMS experiments, often referred to as PIXEAMS, is a useful and an economic alternative as small tandem accelerators

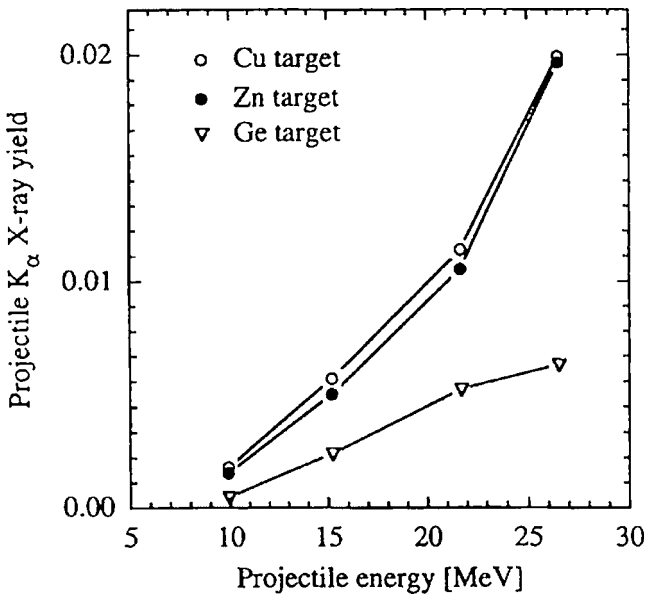

FIGURE 7. The total number of projectile K_α X-ray photons produced per ^{58}Ni projectile as a function of the projectile energy for three different targets. Lines are drawn only to guide the eye. (Reprinted from Wiebert et al. (1996), copyright 1996, with permission from Elsevier.)

can be used instead of larger and more sophisticated methods. At the Lund Pelletron the PIXEAMS technique has been used to measure ^{59}Ni isotopes in steel samples from the nuclear power industry (with isotope ratios, ^{59}Ni/Ni, of 10^{-7}–10^{-10}). For information on the use of PIXEAMS in environmental studies, see Section IVD. The same technique has also been used for ^{36}Cl, ^{60}Fe, ^{63}Ni, ^{79}Se, and ^{126}Sn at a number of different laboratories.

6. *Sample Preparation*

a. Carbon-14. ^{14}C measurements using AMS require that the sample be transformed into elemental carbon in order to produce a stable ion beam with negligible memory effect in the ion source. In the early days of AMS many processes were used for elemental carbon preparation, such as piston cylinder graphitization (Bonani et al., 1984) and cracking of carbon monoxide (Grootes et al., 1980) or acetylene (Beukens & Lee, 1981). The most common method used today is based on the production of elemental carbon by the catalytic reaction of CO_2 over an iron-group metal powder. Vogel and co-workers (1984) were the first to employ this method for AMS measurements. A number of modifications have since been suggested to improve this procedure: reducing the reaction time by, for example, forced gas circulation (Hut, Östlund, & van der Borg, 1986) or using a small reaction volume and higher starting pressure (Lowe & Judd, 1987). The graphitization process is still being improved and methods to reduce the sample size and to minimize background levels are being developed. See, for example Czernik and Goslar (2001); Santos et al. (2004); and Ertunç et al. (2005). Another important aspect is high throughput in sample preparation processes, especially when using AMS for quantitative isotope ratio analysis in the biosciences, where the number of measurements is often very high and the time available for each AMS analysis is short. A method for the rapid production of graphite from biochemical samples has been developed by Vogel (1992), and a refinement of the technique was presented by Ognibene, Bench, and Vogel (2003).

The procedure for converting organic samples to graphite targets at the Lund Radiocarbon Dating Laboratory is outlined below.

Before combustion of the organic samples to be dated they are first chemically prepared to remove any contaminants. Many samples from terrestrial environments, such as wood, charcoal, macrofossils and peat, will often contain small amounts of absorbed carbonates from percolating groundwater. Samples may also absorb humic acids (mobile decay products of biological materials), which are deposited in the vicinity of the sample matrix. Samples contaminated with carbonates often appear too old, while samples contaminated with humic acids often appear too young. To remove these substances the three-step acid-alkali-acid (AAA) method is used. The sample is washed in hot diluted HCl followed by hot diluted NaOH solution. The NaOH may absorb CO_2 from the surrounding air. The final HCl wash ensures that any such contamination is removed. Between each step the sample is rinsed to neutral pH with de-ionized water.

After the pretreatment the samples are combusted and converted to CO_2 using copper(II)oxide as oxidizing agent. For carbonate samples (e.g., mollusks and foraminifers), the carbon dioxide is released by hydrolysis using phosphoric acid.

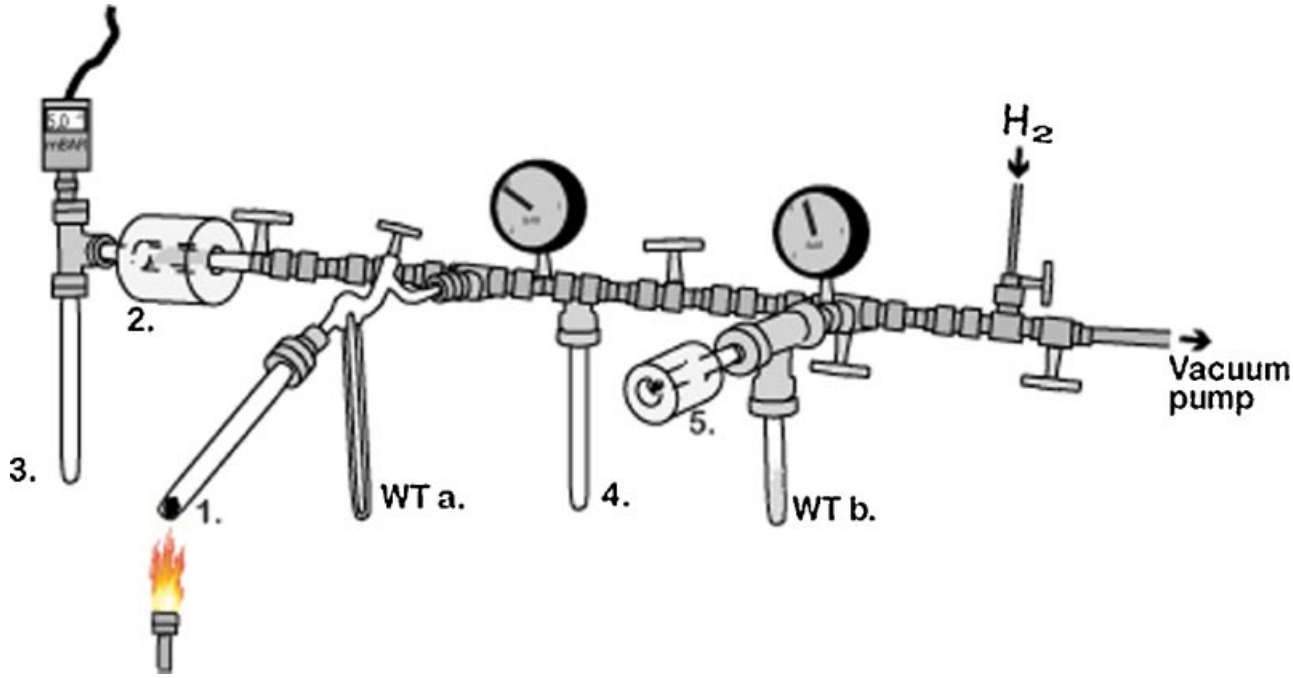

FIGURE 8. The combustion and graphitization system at the Lund Radiocarbon Dating Laboratory. 1. Heating of the sample—CuO mixture; 2. Oven at ~500°C with $PbCrO_4 + Ag$; 3. and 4. Cold traps at liquid nitrogen (LN_2) temperature; 5. Oven at ~600°C with Fe catalyst; WT a. Water trap at approximately 20°C; WT b. Water trap containing $Mg(ClO_4)_2$ as drying agent. [Color figure can be viewed in the online issue, which is available at www.interscience.wiley.com.]

Bioscience samples sometimes require a modified treatment for the release of CO_2 (see for example Persson (1997)). In the form of CO_2 the sample is transferred to a small reaction volume for graphitization.

The combined combustion and graphitization system (see Fig. 8), which is constructed of glass and stainless steel, is connected to a turbo-molecular pump backed by an oil-free membrane pump to evacuate the system. By using dry pumps any carbon contamination from oil pumps is avoided. The metal tubing is heated to approximately 80°C to achieve a lower pressure and to maximize the removal of contaminants. The system is evacuated to below 5×10^{-2} Pa before combustion is started. The process starts by combusting the sample at (1). Water that is produced in the process is trapped at WT a. The released CO_2 gas passes through oven (2), which acts as a trap for impurity gases, and the CO_2 is then trapped at (3) using LN_2. Any remaining contaminants are here removed by pumping on the frozen CO_2 gas for a few minutes. After pumping the CO_2 is released at (3) and trapped again at (4). The CO_2 is released again and the pressure is measured to determine the size of the sample (4). The CO_2 is then transported to the oven at (5) (WT b is temporarily cooled to LN_2 temperature), where it is mixed with H_2 gas. The catalytic Bosch reaction (Manning & Reid, 1977) is used, which can be summarized as:

$$CO_2 + 2H_2 \xrightarrow[\text{Catalyst(Fe)}]{550-650^\circ C} C + 2H_2O$$

The reaction takes place as two successive reduction steps: first to carbon monoxide and then to carbon, which is formed on top of the hot Fe catalyst. The reaction is forced to the right by trapping the produced water at WT b. The time required to complete the reaction is typically around 4 hr.

b. Terrestrial, in situ cosmogenic nuclides. Cosmogenic nuclides produced in the earth's crust (e.g., ^{10}Be, ^{14}C, ^{26}Al, and ^{36}Cl) can require more than 4 weeks of sample preparation because of the time necessary to concentrate the target mineral phases (quartz or other desired minerals) from the sample, and the time required to extract the radioisotopes from the minerals and prepare them in a form suitable for AMS analysis. The samples are first washed or brushed to remove undesirable organic materials, carbonates, and dust, and then crushed, ground, and/or pulverized and sieved to a suitable grain size (sample- and nuclide-specific). Mineral separation and purification are necessary for most analyses. The samples then undergo chemical or thermal isotope extraction in preparation for analysis.

The goal of the extraction process is to collect as much of the cosmogenic nuclide as possible and to separate it from non-cosmogenic nuclides or nuclides that were not produced *in situ* (e.g., atmospheric ^{10}Be). It is especially important to separate the cosmogenic nuclide from any possible isobars (isotopes of the same mass); for example, ^{10}B is a significant isobar of ^{10}Be which can make the mass spectrometric analysis of ^{10}Be difficult. Contaminants are removed from dissolved samples by collection on ion-exchange columns. The cosmogenic isotopes are then selectively precipitated from solution. Finally, the sample is converted to a form suitable for AMS analysis (see Table 1). In preparing a typical rock sample for AMS measurement, approximately 10^6 atoms of the cosmogenic isotopes ^{10}Be and

^{26}Al are needed from 10^{24} atoms of unwanted rock. In addition, a balance needs to be maintained between a sample with an optimum isotope ratio (e.g., ^{10}Be/^{9}Be in the range 10^{-8}–10^{-14}), and a sample with enough material to allow good counting statistics. For a more complete description of the pretreatment methods for *in situ* cosmogenic isotopes see Gosse and Phillips (2001) and references therein.

c. Atmospherically produced cosmogenic nuclides. The pretreatment is similar for most of the nuclides. For example, when ^{10}Be is extracted from ice the procedure is briefly as follows. Approximately 1 kg of ice is melted in a plastic container, together with approximately 1 mg ^{9}Be carrier. Beryllium is then recovered by passing the water through an ion-exchange resin, elution with HCl, and conversion to BeO pellets (Raisbeck et al., 1978, 1981).

An example of the sample preparation procedure for biological samples labeled with ^{26}Al is given in Faarinen et al. (2001).

III. SOME RECENT TECHNICAL DEVELOPMENTS

A. The Trend Towards Smaller Accelerators

As has been mentioned above, in the case of ^{14}C it is known that its isobar, ^{14}N, does not form stable negative ions. The remaining problem is therefore the destruction of hydrocarbon molecular ions such as $^{13}CH^-$ and $^{12}CH_2^-$.

Until the middle of the 1990s the method used to eliminate molecular background in AMS was to allow the ions to undergo charge exchange at high energy (>2.5 MeV) in the high-voltage terminal of a tandem accelerator, to create charge states of 3+ or higher, where molecular bonds are no longer stable. An AMS facility accelerating ions to several MeV has high investment and running costs due to the size of the installation. The possibility of using an accelerator of lower voltage and a lower charge state after charge exchange would thus make the AMS facility both smaller and cheaper. The pioneering work in this field was done by the IsoTrace group in Toronto, Canada (Lee et al., 1984), but it was not until the end of the 1990s, when it was realized through the work of the ETH group in Zurich, Switzerland, that it was possible to carry out radiocarbon dating using charge states lower than 3+.

In 1997, Suter and co-workers discussed the use of a 0.5–1 MV AMS accelerator, which would operate in the 1+ or 2+ charge state. They laid the groundwork for this development with studies showing that molecular interference could be removed with a higher stripper gas pressure than previously used (Suter, Jacob, & Synal, 1997). Later, they reported the design of a prototype 0.5 MV accelerator that would use the 1+ charge state (Suter, Jacob, & Synal, 2000). These studies resulted in an original design of a 0.5 MV accelerator, constructed at ETH in Zurich in cooperation with the National Electrostatic Corporation (NEC) in Middleton, Wisconsin, USA (Suter et al., 1999).

Several 0.5 MV machines have now been built by the NEC and are operational at the Universities of Poznán, in Poland, and Georgia and California-Irvine, in the USA with additional machines under construction. Gracjar and co-workers (2004) described initial studies on ^{10}Be using a terminal voltage of 600 kV. Using low-energy AMS is a challenge, and the main limiting factor is the interfering isobar ^{10}B. The ^{10}Be was injected as BeO^- and stripped to the 2+ charge state giving a final energy of the $^{10}Be^{2+}$ ions of approximately 1.45 MeV. A stack of carbon foils was placed between the high-energy magnet and the electrostatic analyzer suppressing interfering $^{10}B^{2+}$ by 3 orders of magnitude. The boron background was suppressed by another 5 orders of magnitude using a $\Delta E/E$ gas ionization detector (see Section IIB.5). Fifield, Synal, and Suter (2004) have demonstrated the detection of Pu isotopes using AMS at 300 kV. They achieved sensitivities approaching 10^6 atoms for the various Pu isotopes. Their measurements were made with the 500 kV NEC accelerator at ETH in Zurich.

Recently, Klein, Mous, and Gottdang (2006) reported a 1 MV, compact multi-element AMS system, built by High Voltage Engineering Europe (HVEE) in Amersfoort, the Netherlands and comparable in size to the NEC 0.5 MV machine. Its 1 MV voltage capacity makes it more flexible than the 0.5 MV machine, and it allows measurements of iodine and even plutonium. The authors claim that this system is capable of high-precision, low-background measurements of ^{10}Be, ^{14}C, and ^{27}Al. The first of these HVEE machines is in operation at Seville, Spain and a second system will be installed in Trondheim, Norway.

In 2002, discussions started on the possibility of using even lower terminal voltages, perhaps as low as 200 kV, which would eliminate the need for a costly accelerator. A careful study of the stripping yields at these energies shows that this is feasible. Synal et al. (2004) and Synal, Stocker, and Suter (2007) recently presented the results of some test experiments on a 200 kV tandem accelerator. They reported that a background $^{14}C/^{12}C$ ratio of $0.4–1.3 \times 10^{-14}$ could be obtained with the instrument, suggesting that it could be useful for radiocarbon dating.

In 2004, Schroeder and co-workers (2004) discussed the design of another accelerator, with a standard accelerator tube section, but without any pressure tank, which has been built and installed at Lund University. The tank could be eliminated since the high voltage can be sustained in air. This technique is called ''single stage'' AMS (SSAMS), alluding to the fact that the two-step tandem accelerator has been replaced by a single acceleration stage. It operates at a maximum voltage of 250 kV. The stripper is maintained at a high voltage and high-energy mass spectrometry is performed following the stripper without any further acceleration. This arrangement gives backgrounds similar to the 0.5 MV machines discussed previously (Skog, 2007) and can thus be foreseen to be a useful tool for biomedical applications, as well as for radiocarbon dating. The Lund SSAMS system, shown in Figure 9, has a dual injector with two 40-sample, multi-cathode ion sources (1), followed by a 45° rotatable spherical electrostatic analyzer (LEESA) (2) and a 90° low-energy bending magnet (LEBM) (3), all at ground potential. The argon gas stripper (6), the 90° high-energy bending magnet (HEBM) (8), the ^{12}C and ^{13}C Faraday cups, the high-energy 90° ESA (HEESA) (9), the sequential post-accelerator deflector (SPAD) (10), as well as the ^{14}C detector, are placed on an insulated deck with a maximum 250 kV potential. With the rotatable LEESA it is easy (within a few seconds) to change between the two ion sources. This unit also improves the energy resolution of the injected beam and limits it to a narrow energy

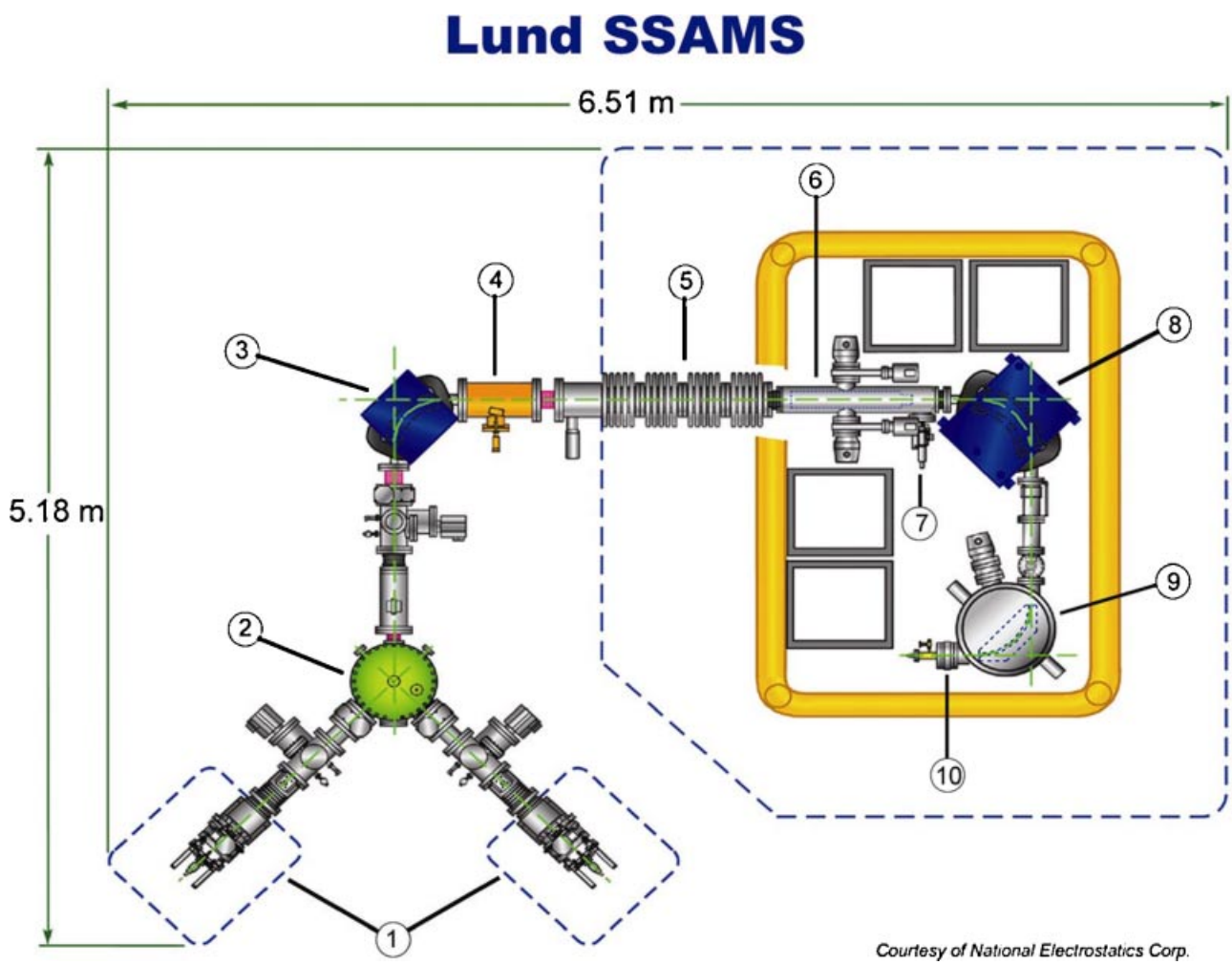

FIGURE 9. The SSAMS system at Lund University. 1. Ion sources; 2. low-energy 45° spherical electrostatic analyzer (LEESA); 3. low-energy bending magnet (LEBM); 4. einzel lens; 5. accelerator tube; 6. argon gas stripper; 7. argon valve; 8. high-energy bending magnet (HEBM); 9. high-energy electrostatic spherical analyzer (HEESA); 10. sequential post-accelerator deflector (SPAD). [Color figure can be viewed in the online issue, which is available at www.interscience.wiley.com.]

range. The carbon isotopes are injected sequentially (see Section IIB.2) with the vacuum chamber of the LEBM biased to preset voltages (~0.2 kV for ^{14}C, ~3.5 kV for ^{13}C, and ~7 kV for ^{12}C). An offset Faraday cup is placed after the LEBM to measure the $^{12}C^-$ and $^{13}C^-$ currents when the ^{14}C isotopes are accelerated. An einzel lens (4) is placed close to the acceleration tube (5) to focus the beams through the molecule-dissociating gas stripper. The mass 14 beam is further energy analyzed by the 90° HEESA (9), and $^{14}C^+$ ions are detected in a surface barrier detector. The $^{12}C^+$ and $^{13}C^+$ beams are energy analyzed and the currents are measured in two Faraday cups after the HEBM (8). The SPAD (10) consists of two parallel plates that deflect the beam upwards when ^{14}C is injected, and downwards when ^{12}C and ^{13}C are injected. The ^{14}C detector is placed at the end of the beam line, displaced by a small angle upwards relative to the beam line. More technical details of the SSAMS system design can be found in Klody et al. (2004). Results from measurements in Lund during 2006 on known standards are given in Table 3. The results are quite close to the consensus values, but the scatter in the data are slightly larger than the statistically expected values.

Data on the typical system performance for the SSAMS in Lund are given in Table 4. Compared to the compact 0.5 MV system, the SSAMS requires approximately 40% less floor space and the investment cost is approximately 30% lower. Furthermore, the SF_6 gas handling system (see Section IIB.3) is avoided, and there is free access to every part of the system (when the high-voltage power is switched off).

B. Attempts at Using Other Types of Accelerators for AMS

As was described in detail in Section II above, by far the largest number of AMS investigations have been made using electrostatic tandem accelerators. Other types of systems have been used in only a limited number of investigations. A great

TABLE 3. Lund SSAMS reference samples measured during operation of the accelerator from May 2006 to January 2007

Meas. no.	*C7/OxII*	*OxI/OxII*
1	0.36915	0.78275
2	0.36773	0.78178
3	0.36944	0.78401
4	0.36773	0.77007
5	0.37593	0.77313
6	0.36885	0.78088
7	0.36862	0.77633
8	0.37153	0.77663
9	0.36833	0.77581
10	0.37071	0.77872
11	0.36728	0.77865
12	0.37124	0.77342
13	0.36989	0.77298
14	0.37019	0.77447
15	0.36915	0.77477
16	0.36855	0.77745
17	0.36922	0.77551
18	0.36848	0.77917
19	0.37101	0.77574
20	0.37086	0.77798
Mean value	0.36969 ± 0.00043 (0.00033)	0.77701 ± 0.00080 (0.00052)
Consensus value	0.3694	0.77563

The two columns show ^{14}C activity ratios, corrected for isotopic fractionation, for the IAEA reference material C7 and the oxalic acid standards OxI and OxII. The numbers in parentheses are the uncertainty arising from the counting statistics only. The total error for an individual measurement is approximately 5‰, corresponding to an uncertainty in age of ±40 years. The consensus values obtained from control measurements at a large number of laboratories are also given.

advantage of the tandem accelerator is that it uses negative ions from the ion source, thus avoiding many interfering isobars (such as $^{14}N^-$ in the case of ^{14}C-AMS). Furthermore, tandem accelerators are widespread and available in many nuclear physics laboratories, they can accelerate nearly all ion types, and they have a better energy stability than any other type of accelerator. For further details about different types of accelerators see Hellborg (2005).

Single-ended electrostatic accelerators have been used in a few attempts, mainly for tritium ions. This type of machine has the ion source at high-voltage potential inside the accelerator tank. It accelerates positive ions from the source and is therefore not very practical for AMS.

Linear accelerators have been used either alone, or as a booster to increase the energy of beams from a tandem accelerator or a cyclotron. In a linear accelerator a number of

TABLE 4. Lund SSAMS system performance data

Ion source output	30 μA of $^{12}C^-$
Transmission	30%
Background (chemical blank)	0.25% of Modern Standard
Background (processed anthracite)	0.4% of Modern Standard
Dating precision (0–6000 BP)	0.6% or ~ ± 50 Radiocarbon Years BP

Transmission is defined as the ratio between the $^{12}C^+$ current after the HEBM and the $^{12}C^-$ current after the LEBM. BP = Before Present, which means before A.D. 1950.

radio frequency (RF) power supplies in succession accelerate bunches of ions. Only ions with the correct velocity will be accelerated, while others will be removed as they reach the different accelerating gaps at the wrong time. The long-lived rare gas isotopes ^{39}Ar and ^{81}Kr (which cannot be made negative and therefore cannot be accelerated in a tandem accelerator) have been used in a GeV energy accelerator (Collon et al., 1997, 2004). Using the high energy of a linear accelerator, it is possible to completely strip these ions. The advantage is that the charge of the rare isotope is now different from that of the isobars, making them easy to separate. The disadvantage is the low efficiency.

Radio frequency quadrupole accelerators (*RFQ accelerators*) have been used in a few attempts to measure tritium and ^{14}C. The RFQ is a low-energy accelerator introduced during the 1970s. It has a high transmission, close to 100%, and with a possibility to handle high currents. The RFQ has a symmetry corresponding to that of an electrostatic quadrupole lens. For technical details see Hellborg (2005). It combines the action of focusing and bunching the beam, in addition to its acceleration property. The acceleration can be continuous (even if most RFQ accelerators are designed for pulsed mode) and the bunching is very efficient. The advantages are: the RFQ accelerator can be made very short (<1 m); it needs no isolation gas and has a much higher current output than a tandem accelerator; also, both the ion source and the detector system are at ground potential so its operation and maintenance are much easier. A well designed RFQ accelerator has a low energy spread and a high isotopic selection (Guo et al., 2007).

Cyclotrons have been used in a number of attempts to measure ions using AMS. Alvarez and Cornog (1939) used one of the pioneering cyclotrons in Berkeley, USA already in 1939 to accelerate helium, when they accidentally discovered the isotope ^{3}He in nature. A cyclotron was also used at the beginning of the AMS era (Muller, 1977). In Shanghai a purpose-built, low-energy cyclotron using negative ions has been demonstrated to have unique mass resolution. The isobars ^{14}C and ^{13}CH, with a mass difference of 5×10^{-4}, can be resolved (Chen et al., 1995), and the first ^{14}C datings were reported a few years ago (Chen et al., 2000; Zhou et al., 2000). The final energy of the beam is very low, only 50 keV. After less than approximately 70 cyclotron revolutions, the isobars $^{12}CH_2$ and ^{13}CH are out of phase due to their mass difference compared to ^{14}C, and are therefore lost. A low-background ^{14}C beam is obtained after the final 100th revolution. The Shanghai mini-cyclotron has recently been upgraded in various ways and provided with a multi-sample Cs sputtering source, similar to those used at most tandem accelerators (Liu et al., 2007).

C. AMS Facilities Worldwide

Tandem-AMS can be said to originate with the observation by Purser and co-workers (1977) that the $^{14}N^-$ ion is not sufficiently long-lived to permit its acceleration in a tandem accelerator. Shortly after this demonstration, the first two AMS experiments followed, at the nuclear physics laboratories at Rochester in the USA (Nelson, Korteling, & Stott, 1977) and McMaster in Canada (Bennett et al., 1977). Only a few years after the introduction of AMS, the first generation of small, dedicated AMS facilities produced by General Ionex Corporation appeared on the market (Purser, Liebert, & Russo, 1980). They are called Tandetrons and are designed on the cascade principle. This first generation of Tandetrons had a maximum reliable operation voltage of around 2 MV. A re-circulating stripping gas system was added to reduce the stripper gas in the accelerator tubes. In 1990 the second generation of Tandetrons, with terminal voltages up to 3 MV, became available (Purser, Smick, & Purser, 1990). Several new AMS facilities based on 3 and 5 MV Pelletrons from NEC have been established during the past few years.

In parallel with this development of new accelerators, older, small machines (up to 3–4 MV) have been modified to serve as AMS facilities. Also, a number of large, tandem accelerators formerly used for nuclear physics have been modified for AMS. In fact, some of these large tandems have been shipped around the world to be assembled at new locations as dedicated facilities. The number of AMS laboratories around the world, completely or partially dedicated to AMS, is approximately 80. Most of these AMS accelerators are listed in Table 5. The radionuclide most frequently measured by far with AMS is ^{14}C. Most of the ^{14}C measurements are performed using accelerators with terminal voltages of approximately 3 MV. Developments using a much smaller voltage started 10 years ago (see Section IIIA) and radiocarbon dating is today done using 0.25 MV accelerators. A few such accelerators are included in Table 5.

Two commercial companies today offer complete AMS facilities: HVEE and NEC.

TABLE 5. Accelerators used solely or partially for AMS around the world

Country	Institute, location	Voltage (MV)/type of accelerator/year of installation/dedicated	Radioisotopes
EUROPE			
Austria	VERA Lab, Univ. of Vienna	3/Pel/95/yes	^{10}Be, ^{14}C, ^{26}Al, ^{36}Cl, ^{41}Ca, ^{55}Fe, ^{129}I, ^{182}Hf, ^{210}Bi, ^{236}U, ^{244}Pu
Denmark	Inst. of Physics and Astronomy, Univ. of Aarhus	6/EN/<90/yes	^{14}C
Finland	Accelerator Lab, Univ. of Helsinki	5/tandem/<90/no	^{14}C
France	ARTIMES, CEA, Gif-sur-Yvette	3/Pel/02/yes	^{14}C
	CEREGE, Marseille	5/Tande/06/…	^{10}Be, ^{26}Al, ^{36}Cl, ^{129}I
Germany	Forschungszentrum, Rossendorf, Dresden	0.1/tandem/…/yes	^{3}H
	Leibniz-Labor, Univ. of Kiel	3/Tande/95/yes	^{14}C
	Max Planck Inst. for Biochemistry, Jena	3/Tande/…./…	^{14}C
	Inst . of Physics, Univ. of Erlangen	6/EN/<90/no	^{14}C
	Maier-Leibnitz Labor, Univ. of Munich	14/MP/<90/no	^{26}Al, ^{36}Cl, ^{41}Ca, ^{53}Mn, ^{59}Ni, ^{60}Fe, ^{63}Ni, ^{129}I ^{182}Hf ^{244}Pu
Italy	Dept of Physics, Univ. of Florence	3/Tande/05/…	^{10}Be, ^{14}C, ^{26}Al, ^{129}I
	Dept of Engineering and Innovation, Univ. of Lecce	3/Tande/02/yes	^{14}C
	Circe, Univ. of Naples, Caserta	3/Pel/05/yes	^{10}Be, ^{14}C, heavy isotopes
the Netherlands	Centre for Isotope Research, Univ. of Groningen	3/Tande/94/yes	^{14}C
	Inst. for Subatomic Physics, Univ. of Utrecht	6/EN/<90/no	^{10}Be, ^{14}C
	Centre for Ion Beam Analysis, Univ. of Utrecht	5-6/Tande/06/...	^{10}Be, ^{14}C, ^{26}Al, ^{36}Cl, ^{129}I
Norway	Univ. of Trondheim	1/Tande/06/yes	^{10}Be, ^{14}C, ^{26}Al
Poland	Radiocarbon Lab, Adam Mickiewics Univ., Poznán	0.5/Pel/01/yes	^{14}C
Romania	National Inst. of Nuclear Physics and Eng., Bucharest	8/FN/<90/no	^{26}Al, ^{129}I
Spain	Centro Nationale de Aceleradores, Seville	1/Tande/06/yes	^{10}Be, ^{14}C, ^{26}Al,
Sweden	GeoBiosphere Science Center, Lund University	0.25/SSAMS/04/yes	^{14}C
	Tandem Lab, Uppsala University	5/Pel/99/no	^{10}Be, ^{14}C, ^{129}I
Switzerland	Inst. of Particle Physics, ETH/PSI, Zurich	0.25/tandem/02/no	^{14}C
		0.5/Pel/99/no	^{10}Be, ^{14}C, ^{26}Al, ^{41}Ca, ^{236}U, ^{244}Pu
		6/EN/<90/no	^{10}Be, ^{14}C, ^{26}Al, ^{36}Cl, ^{41}Ca, ^{59}Ni, ^{60}Fe, ^{126}Sn, ^{129}I
UK	Glaxo-Smith-Kline, Ware near London	0.25/SSAMS/05/yes	^{14}C
	Radiocarbon Accelerator Unit, Oxford University	3/Tande/02/yes	^{14}C

(*Continued*)

	Xceleron Ltd, York Biocenter, Heslington	0.25/SSAMS/in manufa/yes	^{14}C
		5/Pel/98/yes	^{14}C, ^{41}Ca, ^{129}I
	SUERC, East Kilbride, near Glasgow	0.25/SSAMS/07/yes	^{14}C
		5/Pel/02/yes	^{10}Be, ^{14}C, ^{26}Al, ^{36}Cl, ^{41}Ca, ^{129}I
	CHRONO Center, Queen's University, Belfast	0.5/Pel/07/yes	^{14}C
NORTH AMERICA			
Canada	IsoTrace Lab, Univ. of Toronto	2.5/Tande/<90/yes	^{10}Be, ^{14}C, ^{26}Al, ^{129}I, ^{236}U, trace elements
USA	Glaxo-Smith-Kline, Upper Merion, PA	0.25/SSAMS/05/yes	^{14}C
	Beta Analytic, Miami, FL	0.25/SSAMS/05/yes	^{14}C
	Center for Applied Isotope Studies, Univ. of Georgia, Athens,	0.5/Pelle/00/yes	^{14}C
	Dept. Earth Syst. Science Univ. of California at Irvine	0.5/Pel/02/yes	^{14}C
	Accium Biosciences, Seattle, WA	0.5/Pel/06/yes	^{14}C
	Biomed. AMS, MIT, Cambridge, MA	1.0/tandem/01/yes	^{3}H, ^{14}C
	NOSAMS, Woods Hole Oceanographic Institute, MA	0.5/Pel/05/yes	^{14}C
		2.5/Tande/<90/yes	^{14}C
	NSF AMS facility, Univ. of Arizona, Tucson	2.5/Tande/<90./yes	^{10}Be, ^{14}C
		3/Pel/00/yes	^{10}Be, ^{14}C, ^{129}I
	Naval Research Lab, Washington, DC	Pel	^{14}C, trace elements
	Ion Beam Modification Analysis Lab, Univ. N Texas, Denton	3/Pel/<90/no	Trace elements
	PRIME Lab, Purdue Univ. of West Lafayette, DS?	9/FN/91/yes	^{10}Be, ^{14}C, ^{26}Al, ^{36}Cl, ^{41}Ca, ^{129}I
	Lawrence Livermore National Lab, CA	1.0/Pel/99/yes	^{3}H, ^{14}C
		9.5/FN/…./yes	^{10}Be, ^{14}C, ^{26}Al, ^{36}Cl, ^{41}Ca, ^{63}Ni ^{236}U ^{237}Np ^{244}Pu
	Oak Ridge National Lab, Oak Ridge, TN	25/Pel/<90/no	^{36}Cl
	ATLAS facility, Argonne National Lab, DS?	Supercond Linac/<90/no	^{39}Ar, ^{63}Ni, ^{182}Hf, ^{236}U, ^{244}Pu
MIDDLE EAST			
Israel	Physics Dept, Weizmann Institute, Rehovot	14/Pel/<90/no	^{7}Be, ^{10}Be, ^{14}C, ^{26}Al, ^{36}Cl, ^{41}Ca, ^{44}Ti, ^{59}Ni, ^{90}Sr, ^{129}I, ^{236}U, $^{239,240,242,244}Pu$,
ASIA			
China	Mini-cyclotron, Shanghai Institute of Nuclear Physics	50 keV/cyclotron/98/yes	^{14}C
	Inst. Earth Env, Chinese Acad. of Science, X'ian	3/Tandc/06/…	^{10}Be, ^{14}C
	Inst. of Heavy Ion Physics, Peking University	0.5/Pel/04/yes	^{14}C

TABLE 5. (*Continued*)

		6/EN/<90/…	^{10}Be, ^{14}C
	Chinese Institute of Atomic Energy, Peking	13/MP/<90/no	^{36}Cl, ^{41}Ca, ^{79}Se
India	Multidisciplinary Research Accelerator, Inst of Physics, Bhubaneswar	3/Pel/<90/no	^{14}C
	Nuclear Science Center, New Delhi	15/Pel/<90/no	^{10}Be, ^{36}Cl
Japan	Paleo Labo Co. Ltd, Kurahone, Kiryu	0.5/Pel/04/yes	^{14}C
	Institute for Applied Accelerator Analysis, Kanagawa	0.5/Pel/05/yes	^{14}C
	Dating and Material Research Center, Nagoya University	2.5/Pel/97/yes	^{10}Be, ^{14}C
		3/Tande/<90/yes…	^{14}C
	Inst for Applied Accelerator Analysis, Kanagawa	3/Pel/00/yes	^{10}Be, ^{14}C
	Marine Research Lab, Japanese Atomic Energy Inst., Mutsu	3/Tande/…/…	^{14}C, ^{129}I
	Tono Geoscience Center, JAEA, Toki Gifu	5/Pel/97/yes	^{10}Be, ^{14}C
	Research Center for Nuclear Science and Technology, Univ. of Tokyo	5/Pel/92/no	^{10}Be, ^{14}C, ^{26}Al
	National Inst for Environmental Studies, Tsukuba	5/Pel/95/yes	^{14}C
	Dept of Physics, Kyoto University	8/Pel/<90/no	^{14}C
	Dept of Physics, University of Kyushu, Fukuoka	10/tandem/…/…	^{14}C, ^{36}Cl
	Tandem Accelerator Center, Univ. of Tsukuba	12/Pel/<90/no	^{36}Cl
Russia	Budker Institute for Nuclear Physics, Novosibirsk	2/tandem/under test/yes	^{14}C
South Korea	Dept of Physics, Seoul National University	3/Tande/99/no	^{10}Be, ^{14}C
AUSTRALASIA			
Australia	Nuclear Physics Dept, Australian National Univ., Canberra	0.25/SSAMS/07/yes	^{14}C
	STAR at ANSTO, Menai, Sydney	2/Tande/04/no	^{14}C
	ANTARES at ANSTO, Menai, Sydney	8/FN/91/no	^{10}Be, ^{14}C, ^{26}Al, ^{129}I, ^{236}U, ^{239,240}Pu
	Nuclear Physics Dept, Australian National Univ., Canberra Group together!	14/Pel/<90/no	^{10}Be, ^{14}C, ^{26}Al, ^{36}Cl, ^{41}Ca, ^{59}Ni, ^{99}Tc, ^{129}I, ^{182}Hf, ^{236}U, ^{237}Np, ^{244}Pu
New Zealand	Isotope Center, Inst. of Geology & Nuclear Science, Lower Hutt	6/EN/<90/yes	^{10}Be, ^{14}C, ^{26}Al
SOUTH AMERICA			
Argentina	TANDAR, National Atomic Energy Com, Buenos Aires	20/Pel/<90/no	^{36}Cl
Brazil	Nuclear Physics Dept, University of Sao Paolo	9/Pel/<90/no	^{36}Cl
AFRICA			
Egypt	Atomic Energy Agency, Anshas, Cairo	3/Tande/…/…	^{14}C

"Pel" is an abbreviation for Pelletrons produced by NEC. "Tande" is an abbreviation for Tandetrons produced by HVEE (and originally by General Ionex). SSAMS is a small AMS-dedicated accelerator produced by NEC. Models EN, FN, and MP are nuclear physics tandem accelerators produced during the 1960s and 1970s by HVEC Burlington, USA. Year of installation and whether or not the accelerator is dedicated to AMS are given in column 3 (if known). "<90" is used to denote installation before 1990.

IV. APPLICATIONS

A. Archeology and Geology

1. Calibration of the Radiocarbon Time Scale

The radiocarbon method is based on the rate of decay of the radioactive carbon isotope ^{14}C, which is formed in the upper atmosphere through the reaction between cosmic ray neutrons and ^{14}N: $n + {}^{14}N => {}^{14}C + p$, where n is a neutron and p is a proton. The ^{14}C atoms are rapidly oxidized to $^{14}CO_2$ molecules which are taken up by plants. ^{14}C is further transported to animals through the food chain. Thus, plants and animals take up radioactive carbon while alive, but cease to do so when they die. However, the steady decay of ^{14}C in their tissues continues over the years. The ^{14}C atoms decay back to ^{14}N, with a half-life of ca. 5,700 years, according to the reaction: $^{14}C => {}^{14}N + \beta$, where β is an electron (also called beta radiation) emitted by the ^{14}C nucleus. After nine half-lives, which corresponds to ca. 50,000 radiocarbon years BP, we have ca. 2‰ ^{14}C left in the sample. The detection limit of ^{14}C for an AMS facility is 1–2‰ of modern carbon (corresponding to a $^{14}C/^{12}C$-ratio of around 10^{-15}), which sets an upper limit for the radiocarbon method to slightly above 50,000 years.

The intensity of the cosmic radiation on earth varies with the sun's solar activity and fluctuations in the earth's magnetic field, and thus the production of ^{14}C in the atmosphere also varies. Moreover, the uptake of carbon dioxide in the oceans varies with changes in the ocean ventilation rate when the earth's climate changes rapidly. This means that the radiocarbon level in the atmosphere changes according to a complex pattern, which in turn means that the ''radiocarbon clock'' can race ahead or sometimes stop for several centuries, and even go backwards. As a result, a raw radiocarbon date may correspond to several possible calendar dates, and may diverge from real calendar years by hundreds or even thousands of years. Thus, the radiocarbon clock must be calibrated to account for these fluctuations. For example, the start of the Holocene period, the period in time when the last ice age ended, is dated to 10,000 radiocarbon years ago. But the radiocarbon clock stopped for several hundred years at just that point, so the start of the Holocene, when agriculture began, cannot be determined with better precision than approximately 600 years using the radiocarbon method alone. Using the tree-ring radiocarbon calibration curve (see below) this transition has been shown to occur somewhere between 11,800 and 11,200 years ago.

Recent research to determine the pattern of fluctuation of the ^{14}C content of the earth's atmosphere has led to better and more detailed calibration curves for the past 50,000 years. Using ^{14}C data from tree rings, corals, lake sediments, ice cores, and other sources, the radiocarbon community has now created a detailed record of ^{14}C variations over the millennia and extended the ''official'' radiocarbon calibration curve back 26,000 calendar years (Reimer et al., 2004). Of these data records, the terrestrial tree-ring curve, extending back 12,400 years is the most accurate and precise. The tree-ring curve is based on several millennia-long chronologies, providing an absolute time frame within the possible error of dendrochronology. These long chronologies come from wood from Europe and North America (see for example Stuiver, 1982; Pilcher et al., 1984; Becker & Kromer, 1986; Pearson, Becker, & Qua, 1993; Spurk et al., 1998). The oldest part of the tree-ring chronology has been constructed from German pine, and has been successfully linked to the younger German oak chronology (Friedrich et al., 2004).

Beyond the tree-ring curve, the calibration data sets rely mainly on marine samples (van der Plicht et al., 2004). Although the discrepancy between the different datasets in the time interval 26,000–50,000 radiocarbon years BP is rather large, they all show that the calendar time scale sets the radiocarbon clock back several thousand years in this interval. The data sets come from radiocarbon dating of a sequence of deep-sea sediments in the Cariaco Basin near Venezuela, and from a similar sequence of dating from deep-sea sediments adjacent to the Iberian coast. These sequences were translated into a ''calendar'' scale by reference to patterns of oxygen isotopes ($^{18}O/^{16}O$) in the Greenland ice core records. The data sets also include series of radiocarbon and uranium/thorium (U/Th) measurements on fossil coral formations from the tropical Atlantic and Pacific and from a sequence of a cave stalagmite formations on the island of Socotra, off the Arabian coast (Hughen et al., 2004; van der Plicht et al., 2004; Fairbanks et al., 2005).

The final goal, which is to extend the tree-ring calibration curve to 50,000 years, probably lies several decades ahead.

2. Calibration with the ^{14}C Bomb Peak

Nuclear weapon testing in the atmosphere caused in the 1960s almost a doubling of the ^{14}C activity in the atmosphere. After the stop of these nuclear tests in the atmosphere the peak started to decrease through interaction of the atmosphere with the other carbon reservoirs. Today (2007) the remaining ''excess activity'' is around 6%. Samples originating from the time period after ca. 1955 can be radiocarbon dated utilizing the ^{14}C bomb peak as a calibration curve. Clearly, the ^{14}C-bomb peak can be used to retrieve very precise dates (within 1 year at the steepest part of the curve, i.e., during the 1960s and 1970s; Goodsite et al., 2001). Another example of such an application is given in Section IVC.2.

3. Dating of Lake Sediments

The common method of dating in quaternary geology and paleoclimatology studies is to use the archives of lake sediments. An important question is the chronology of the cores that are taken from the lakes. Earlier studies were based on large bulk sediment samples, mainly consisting of gyttja (as much as 100 g of wet material or 5 g of dry material were common). Gyttja is made up of organisms that have lived in the lake and have taken their carbon from the lake water. The lake reservoirs contain carbon from many different sources: dissolved limestone, humic acid from soil and peat in the surroundings, or carbon dioxide from ''old'' ground water reservoirs. Of course, a large part also comes from carbon dioxide exchanged with the atmosphere at the lake surface. However, the radiocarbon level in the lake does not reflect the contemporary atmosphere and, therefore, we have the

problem of the so-called lake reservoir age, which gives older dates than expected from the atmospheric record.

Before AMS was established, the problem of ''hard-water'' lakes was well known, and dating lakes with limestone in the surrounding bedrock was avoided. However, AMS dating showed that the reservoir problem was also severe for ''soft-water'' lakes. Instead of dating whole bulk samples it was now possible to date small macrofossils from the vegetation around the lake, samples that reflect the atmospheric level of radiocarbon rather than the level in the lake. This has been a very important development for quaternary geologists and has led to completely new sampling techniques.

This is clearly demonstrated in an investigation that partly deals with the tree limit in ancient times in the Scandes Mountains in northern Sweden and Norway (Barnekow, Possnert, & Sandgren, 1998). The radiocarbon chronology in this investigation was very carefully determined, both with terrestrial macrofossils found in the cores and with bulk gyttja samples. The investigation was performed in a ''hard-water'' lake (Lake Tibetanus) and a ''soft-water'' lake (Lake Voulep Njakajaure). The results of this investigation and other studies, for example Andrée et al. (1986), clearly demonstrated the importance of selecting the correct material for radiocarbon dating. The terrestrial macrofossils gave younger ages than the bulk samples in all cases. The reservoir age in Lake Tibetanus can be estimated to be 1,000–2,000 years, and furthermore it varies with time. In Lake Voulep Njakajaure the reservoir effect is less, but there is still a reservoir age of approximately 500 years. This is quite typical for Swedish ''soft-water'' lakes (Olsson, 1986).

The first results of pollen dating from sediments were obtained by Brown and co-workers (1989). Since then, a number of successful, but also problematic, investigations based on dating of pollen concentrates, with sample sizes in the sub-mg range, have been made, for example Long, Davis, and DeLanois (1992); Regnell (1992); Jahns (2000); Kilian et al. (2002); Vasil'chuk, Kim, and Vasil'chuk (Vasil'chuk et al., 2004). When preparing such small samples there is of course an increased risk of contamination of the sample, and it is especially important to have good knowledge of the background factors. Pollen diagrams are used to trace vegetation and climate changes in the past, and it is of course tempting to try to directly date the pollen itself.

Radiocarbon dating of macrofossils and pollen is not possible without the AMS technique, and it is therefore relevant to talk of a ''second radiocarbon revolution'' in quaternary geology after the introduction of ^{14}C dating with AMS.

4. Atmospheric ^{10}Be

The AMS technique has had considerable influence on radiocarbon dating, but it has had an even greater impact in other fields of quaternary geology, which use the other cosmogenic isotopes. Before 1990, cosmogenic nuclides apart from ^{14}C were more or less unknown to quaternary geologists. This was simply due to the fact that there was no practical way to measure the extremely small concentrations of these cosmogenic nuclides produced in the geological archives. Let us consider ^{10}Be, the most important cosmogenic nuclide apart from ^{14}C. The half-life of ^{10}Be is long enough (1.6 million years) to cover the whole quaternary period. The best archives for ^{10}Be are the marine sediments and the inland ices of Greenland and Antarctica. One kilogram of ice contains approximately 50 million ^{10}Be atoms. Concentrated to a 1 mg substrate, this is an excellent sample for an AMS measurement. Decay counting of ^{10}Be, on the other hand, is virtually impossible due to its long half-life. All the ^{10}Be nuclides in 1 ton of ice would only give approximately 65 counts in 24 hr. Thus, without AMS, the ^{10}Be signal would have remained hidden in the archives.

The ^{10}Be concentration in ice and marine sediments is an indicator of solar fluctuations, which in turn control the cosmic ray flux that reaches the earth from outer space. The more active the sun, the less intensive the cosmic rays on earth, and vice versa. During the period 1,660–1,740 there is a distinct peak in the ^{10}Be record (Beer et al., 1994; Bard et al., 1997). It is known from visual observations that during this period there were hardly any sunspots on the solar surface and the sun remained quiet. Consequently, the cosmic ray intensity increased, as did the ^{10}Be signal. The same is also true for other cosmogenic isotopes such as ^{14}C. The ^{14}C signal is, however, more difficult to interpret as it also depends on the ocean ventilation rate, which determines the amount of carbon dioxide that is dissolved in ocean waters.

By combining data from marine records of the varying production rates of ^{10}Be with data on the variations in the earth's magnetic field intensity, it has proven to be possible to calculate the variations in the solar magnetic activity 200,000 years back in time (Sharma, 2002). This study indicated that the glacial and interglacial periods on earth during the past 200,000 years appear to be strongly linked to solar activity (see also Beer, Mende, & Stellmacher, 2000; Bond et al., 2001). The amount of ^{10}Be was compared to the oxygen isotopic record, which is closely related to the global temperature. The two records follow each other very closely, which is a strong indication that small solar variations may have a great impact on the climate.

Recently, evidence of enhanced ^{10}Be deposition deep in the Antarctic ice was reported (Raisbeck et al., 2006). The authors interpreted this as a result of the low dipole field during the Matuyama–Brunhes geomagnetic reversal, which occurred approximately 780,000 years ago. If this is correct, it will be an important time marker connecting ice cores, marine cores, and radiometric time scales.

5. Exposure Dating

When a bedrock surface is exposed to cosmic rays, a build-up of cosmogenic nuclides will occur within minerals in the uppermost few meters of the rock. The ability of AMS to measure low concentrations of rare cosmogenic nuclides has led to new methods of addressing long-standing geological questions, and has provided new insights into the rates and types of surface processes. The most widely used of the cosmogenic nuclides are the stable isotope ^{3}He and the radioactive nuclides ^{14}C, ^{10}Be, ^{26}Al, and ^{36}Cl. Their different physical and chemical properties make it possible to apply surface exposure dating methods to rock surfaces of virtually any lithology at any latitude or altitude, for exposures ranging from the late Holocene to the Pliocene (>2.65 million years). The terrestrial *in situ* cosmogenic nuclide method is beginning to revolutionize the manner in which landscape evolution is studied. Single or multiple nuclides can be

measured in a rock surface to obtain erosion rates on boulder and bedrock surfaces. A particularly interesting system is the $^{10}Be-^{26}Al$ pair that is produced in quartz, where ^{26}Al is mainly produced from ^{28}Si and ^{10}Be is mainly produced from ^{16}O. The *in situ* produced cosmogenic nuclides from continental and mountain erosion records have been used to reconstruct Quaternary ice volume variations. The *in situ* methods have also been used in significant breakthroughs in establishing the rates and types of local- and large-scale erosion, soil development, and landscape evolution. A complete review of the subject is given in Gosse and Phillips (2001).

6. Recent Developments in Radiocarbon Dating and Archeology

Since its introduction in the early 1950s, the radiocarbon dating method has been an essential tool for archeologists. Collecting charcoal and bones for dating during excavations is standard practice, and systematic dating for research purposes is also becoming more and more common. With AMS it is possible to date short-lived material such as a single grain of wheat or a blade of grass. A small piece of bone of sub-g weight (Hedges & van Klinken, 1992) and also charred bones (Lanting, Aerts-Bijma, & van der Plicht, 2001) can now be dated, which was previously impossible. Analyzing more than one sample from a site or object can give indications of contamination, improving the reliability.

Until quite recently, cave paintings were dated according to stylistic criteria loosely associated with dates obtained from archeological remains found in the vicinity of decorated surfaces. Advances in radiocarbon dating with AMS now make it possible to date prehistoric cave paintings by sampling the pigment itself. The ages obtained from paintings decorating two French caves at Cosquer and Chauvet have so far shown that the art of cave painting appeared early in the Upper Paleolithic period, which is much earlier than previously believed. The high artistic quality of the earliest paintings underlines the importance of absolute chronology in any attempt to study the evolution of prehistoric art. Prehistorians, who have traditionally interpreted the evolution of prehistoric art as a steady progression from simple to more complex representations, may have to reconsider existing theories of the origins of art. In the Chauvet caves, which consist of several chambers, radiocarbon dates of between 29,700 and 32,400 years BP have been obtained for sub-mg charcoal samples (Valladas et al., 2001; Valladas, 2003).

Radiocarbon dating has been applied to the study of modern human origins and dispersal in Eurasia (Mellars, 2006). Recent developments, involving ultrafiltration of the prepared gelatin samples derived from bone collagen to separate out the smaller and lower-molecular-weight fractions (Bronk Ramsey et al., 2004) have led to radical improvements in the procedures for the effective purification of bone collagen to eliminate contamination by more recent carbon. Removing recent contaminants is of special importance in older bone samples, which have always provided the most widely available materials for dating from early human sites. Recent applications of this procedure have led to dates that are frequently between 2,000 and 7,000 years older than the original age estimates (Jacobi, Higham, & Bronk Ramsay, 2006).

These new developments are of crucial importance when trying to determine the time of the extinction of the Neanderthals in Europe. Recently, an international team reported several radiocarbon dates from Gorham's cave in Gibraltar (Balter, 2006). The dates cluster at approximately 28,000 years raw ''radiocarbon years,'' indicating that the Neanderthals survived much longer than previously thought. It is believed that the Neanderthals took refuge in southern Europe where the environment was favorable and where modern humans were still fairly rare.

Art and human history are of general interest and therefore the dating of some objects by AMS has given rise to considerable publicity. The best known cases are the dating of the Turin Shroud (Damon et al., 1989), the Iceman in Ötztal (Bonani et al., 1994), and the Dead Sea Scrolls (Bonani et al., 1992). A ceremonial book from the earliest period of Christianity in Sweden was dated at the Lund AMS laboratory. The book, originating from around A.D. 1100, is regarded as the oldest book in Sweden (Skog, 2002).

B. Oceanography

1. Carbon-14

Natural ^{14}C, which is produced only in the atmosphere, is very useful in understanding deep ocean circulation, because any natural ^{14}C atoms found at depth in the ocean must have arrived there by means of exchange between the atmosphere and the ocean surface water and subsequent transport within the body of water. Because ^{14}C decays with a half-life close to 5,730 years, its abundance in the deep ocean is a direct measure of how much ^{14}C is supplied to the deep ocean from the surface by ventilation. Temperature measurements of deep ocean water reveal that much of the deep water is cold, and warm water is confined to a thin layer near the surface, indicating that the deep cold water in the subtropics must derive from the polar surface waters. This is known as the thermohaline circulation or the ''conveyor belt'' circulation (Broecker, 1991). A description of the conveyor belt has been made possible by AMS ^{14}C measurements.

As part of the World Ocean Circulation Experiment (WOCE) thousands of small-volume water samples were collected and the ^{14}C content of the dissolved CO_2 analyzed by AMS. The samples were collected at various depths along transects across the oceans. Over 13,000 samples were collected during 1990–1997 for this program, and were measured at the National Oceans Science Accelerator Mass Spectrometry (NOSAMS) Laboratory at Woods Hole, Massachusetts, USA. During 1990–2004 more than 8,000 articles were produced as a result of this program. A summary of the results concerning ^{14}C is given in Key et al. (2002).

The main reason for studying deep circulation is that the deep ocean is the major component of the global carbon cycle. The world's oceans contain approximately 93% of all carbon on earth. Since most of the oceanic carbon resides in the deep ocean, even a small change in its carbon budget can significantly affect the atmospheric budget and hence the global climate. The chances of such an event may seem remote, because changes in the deep ocean are slow compared to those in the atmosphere, upper ocean, and terrestrial biosphere. However, measurements

from polar ice cores provide abundant evidence of abrupt climate changes during the most recent glacial cycle (Dansgaard et al., 1993), some of which may have involved changes in the deep ocean (Broecker, 1998, 2003). Abrupt climate change may be a real possibility today, as human activities that modify the physical environment are increasing globally (Broecker, 1997; Alley et al., 2003).

Another important reason for accurately characterizing the deep ocean is the need to validate ocean carbon cycle models. These models are frequently used to predict the response of the ocean to increasing atmospheric CO_2. Projections of future carbon uptake by the ocean (Houghton et al., 2001) inevitably involve the deep ocean. Global mapping of the ^{14}C abundance at 3,500 m depth using the WOCE database, shows the highest concentrations of ^{14}C in the north Atlantic. The north-east Pacific has the lowest ^{14}C concentration, indicating the end of the conveyor belt circulation, while the Southern Ocean (the ocean south of 60°S latitude) has an intermediate ^{14}C concentration. Translating the difference in ^{14}C concentration between the north Atlantic and north-east Pacific deep waters into years reveals an age difference of approximately 1,000 years, which thus characterizes the turnover of the global circulation (Matsumoto & Key, 2004).

2. Iodine-129

Another important radionuclide used as a tracer of marine current movements is ^{129}I. It has a half-life of approximately 16 million years and its presence in nature is mainly due to the fission of ^{235}U and spallation of stable Xe isotopes by cosmic radiation in the atmosphere. The pioneering work on ^{129}I in the ocean was done by Kilius, Rucklidge, and Litherland (1987). ^{129}I can easily be quantified by AMS from iodine extracted from 500 mL seawater. The high sensitivity of AMS enables trace amounts of ^{129}I released from radioactive waste (e.g., from nuclear fuel reprocessing plants) to be detected and local levels to be compared with the global distribution (Povinec et al., 2000, 2001; Yiou et al., 2002). The globally distributed anthropogenic ^{129}I emanates mostly from the nuclear weapons tests of the 1950s and 1960s and has probably been spread to the ocean by atmospheric transport (Biddulph, 2004). Lopez-Guitérrez and co-workers (2000) have developed a method for the determination of ^{129}I in atmospheric samples.

C. Biomedicine

1. General Aspects

The cost and size of conventional AMS accelerators have restricted their penetration into the bio-analytical instrument market. The recently introduced AMS accelerators with voltages well below 1 MV (see Section IIIA), having a much reduced size and complexity, have changed the situation.

Isotopic labeling has been used for many years for tracing chemicals in living systems. Three kinds of labeling can be used. Short-lived radioactive isotopes have a high signal to background ratio, but they have the disadvantage of exposing the organism to radiation. Stable isotopes emit no radiation, but due to an often high natural background they are not easy to detect. Long-lived radioactive isotopes have a high signal to background ratio and can be used in biomedical AMS in very small amounts. Because of their low radioactivity, the radiation to the individual will be kept to a minimum. The radiation dose deposited in a human as a function of the biological mean life has been calculated by Vogel (2000). The result for a 70 kg person who has been given a compound labeled with ^{14}C ($T_{1/2} = 5{,}730$ y) with an activity of 3,700 Bq is shown in Figure 10. The dose obtained during a 1-hr flight and the dose obtained from natural isotopes inside one's own body (^{14}C, ^{40}K, etc.) during a week are also indicated in the figure for comparison. Another advantage of biomedical AMS is the high sample throughput; the measuring time often being less than 10 min/sample.

Accelerator mass spectrometry (AMS) is sensitive and precise to a few attomoles of ^{14}C per gram carbon, which renders a number of advantages to biomedical tracing. The use of such small amounts of material enables the use of sub-toxic amounts of a chemical substance, the analysis of small tissue biopsies or a few μL of blood, as well as the analysis of highly specific biochemical substances and sub-cellular fractions, including purified DNA.

Accelerator mass spectrometry (AMS) has been applied to a number of other long-lived radioisotopes during the past 10–15 years and has been found to be important in research on human biochemistry. Hydrogen is used together with carbon for organic tracing *in vivo* with molecules labeled with ^{3}H ($T_{1/2} = 12.33$ y) and ^{14}C. The $^{3}H/^{1}H$ ratio of a mg-sized water sample can be measured at a level of a few times 10^{-16}, which means that AMS provides a factor of 10^3 improvement in sensitivity with mg-sized ^{3}H-samples compared to decay counting (Ognibene et al., 2004). Aluminum, the most common metal in the earth's crust, is a non-essential element in biological systems. However, it is known to have a deleterious effect on neurological systems. Aluminum is highly neurotoxic and inhibits prenatal and postnatal development of the brain in humans and animals. The introduction of ^{26}Al ($T_{1/2} = 7.16 \times 10^5$ y) as an AMS isotope has enabled the study of aluminum metabolism under physiological conditions. It has been demonstrated that as little as 5 attograms of ^{26}Al can be detected by AMS (Yumoto et al., 2004). Calcium is an important element in the human body. Many diseases are related to calcium in organs and cells. ^{41}Ca ($T_{1/2} = 1.04 \times 10^5$ y) is therefore an ideal tracer. Several studies of calcium have been reported, such as long-term bone resorption, calcium uptake and deposition in heart tissue, and the metabolism of calcium in the skeleton (Jiang et al., 2004).

The more extensive use of AMS in biomedical research will require the development of cost-effective, laboratory-sized AMS systems that can be used in conjunction with gas and liquid phase separation techniques. Considerable progress has recently been made in coupling gas and liquid chromatography directly to AMS to allow on-line, compound-specific ^{3}H and ^{14}C analysis. The ability to directly interface an AMS system to standard analytical instruments would allow AMS to be used for real-time analysis. The interface must provide efficient conversion of a wide variety of biological molecules into the required ion source gas. Through collaboration between the Massachusetts Institute of Technology and a commercial company a gas chromatograph (GC) has

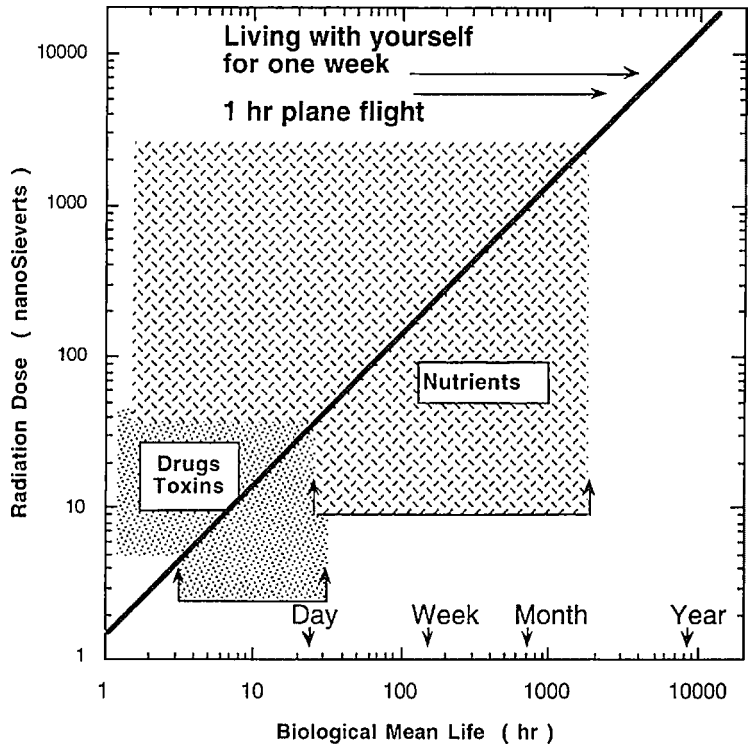

FIGURE 10. The radiation dose deposited in a 70 kg person as a function of the biological mean life of 3,700 Bq in a ^{14}C-labeled compound. An 1-hr plane flight produce the exposure indicated by ''1 hr plane flight'' Natural radioisotopes within an individual produce the exposure indicated by ''living with yourself.'' (Reprinted from Vogel (2000) copyright 2000, with permission from Elsevier.)

been coupled directly to a gas-fed negative ion source to achieve on-line AMS measurements (Hughey et al., 2000). Skipper and co-workers (2004) were the first to demonstrate the operation of a GC and AMS instrument together to detect ^{14}C in labeled compounds. They also presented promising results on a laser-induced combustion interface to connect a high-pressure liquid chromatograph with an AMS ion source. Examples of other AMS laboratories working on such schemes are ORAU (the Oxford Radiocarbon Accelerator Unit) in Oxford, UK (Ramsey, Ditchfield, & Humm, 2004) and the Woods Hole Oceanographic Institute in Massachusetts, USA (Schneider et al., 2004).

An AMS system dedicated to biomedical applications is installed at a commercial company in York, UK. The system is based on a 5 MV tandem accelerator produced by NEC. At the Lawrence Livermore National Laboratory in the USA, a 1 MV tandem and a 10 MV tandem are used for AMS. The smaller accelerator manufactured by NEC is used for ^{3}H and ^{14}C isotopes and the larger accelerator (originally a nuclear physics accelerator from the 1960s, used for many years at another laboratory) is used for the isotopes ^{10}Be, ^{26}Al, ^{36}Cl, ^{41}Ca, ^{59}Ni, ^{63}Ni, ^{99}Tc, ^{129}I, and ^{239}Pu. At the Massachusetts Institute of Technology a 1 MV tandem (built by Newton Scientific, Inc.) is used for ^{14}C studies. Two SSAMS machines (see Section IIIA) were purchased by Glaxo-Smith-Klein to be used for drug development and were installed by the NEC in 2005. One of the machines is placed at Ware in the UK and the other at Upper Merion, Pennsylvania, USA.

2. *Some Specific Applications*

Before the introduction of AMS, biokinetics and radiation dose estimates from radiopharmaceuticals, labeled with pure β-emitting radionuclides, for example, ^{14}C or ^{3}H were very uncertain. The radiation physics group at the Lund University Hospital in Malmö, in cooperation with the Lund AMS group, has carried out detailed long-term biokinetic studies of ^{14}C from ^{14}C-labeled pharmaceuticals in humans. The studies conducted were mainly related to so-called ''breath tests,'' where the ^{14}C-labeled compound is ingested and metabolized, resulting in the end-product, $^{14}CO_2$, which is exhaled and easily collected for measurement.

The AMS technique has been used to study the long-term retention of ^{14}C in connection with clinical tests for the presence of *Helicobacter pylori* in the stomach with ^{14}C-urea. The long-term biokinetics and dosimetry of ^{14}C-urea were investigated in a number of adults and children (Leide-Svegborn et al., 1999) and (Gunnarsson et al., 2002b). It was concluded from the investigation that a dose of 440 Bq is sufficient to obtain useful results, compared to the 110 kBq necessary for scintillation counting. Fat malabsorption of the gastro-intestinal tract was also studied using the ^{14}C-labeled triolein breath test. Measurements were made of the loss of ^{14}C in expired air, urine, and feces, and the retention of ^{14}C in biopsy samples of abdominal fat were made (Stenström et al., 1996c, 1997). Biopsies were taken from body fat, muscles, and bone from one of the volunteers $4\frac{1}{2}$ years

and 6 years after administration (Gunnarsson et al., 2000; Mattsson et al., 2001). It was concluded that no restrictions need to be placed, on radiation safety grounds, on the administration of 0.05–0.1 MBq ^{14}C-triolein for the triolein breath test (Gunnarsson et al., 2003). The ^{14}C-glycocholic acid and ^{14}C-xylose breath tests are used for the diagnosis of intestinal diseases such as bacterial overgrowth in the small intestine. In another study the long-term biokinetics and dosimetry of the two compounds were investigated. Samples of exhaled air, urine and for some subjects also feces were analyzed. The absorbed dose to various organs and tissues and the effective dose were calculated using biokinetic models based on a combination of experimental data from this study and earlier ones. The calculated effective dose was found to be 0.4–0.6 mSv/MBq (for glycocholic acid) and 0.1 mSv/MBq (for xylose). From a radiation protection point of view there is no need for restrictions in the use of these two radiopharmaceuticals with the activities normally administered (0.07–0.4 MBq; Gunnarsson, 2002a).

In conclusion, the use of ultra-low activities in combination with AMS (down to 1/1,000 of those used for liquid scintillation counting), has led to the possibility of metabolic investigations on children, as well as on other sensitive patient groups such as newborns, and pregnant or breast-feeding women. It has been demonstrated that AMS has great potential in the study of metabolism and related areas. In particular, it will enable the administration to humans of very low activities, for example, 10 Bq of ^{14}C. For most substances this will lead to effective doses of less than 1 μSv, which is so low that in many countries authorization from radiation protection authorities is not required.

The generation of cells in the human body has been difficult to study, and the rates of cellular turnover of important cell types within human organs are largely unknown. A new technique has been developed at the Medical Nobel Institute and the Karolinska Institute in Sweden, taking advantage of the sudden and dramatic increase in ^{14}C in the atmosphere resulting from the nuclear weapons tests in the 1950s and 1960s. At the time of the atmospheric Test Ban Treaty in 1963, the ^{14}C content in the atmosphere had increased by a factor of two above the natural level when the test period started. Since the Test Ban Treaty in 1963 there has been an approximately exponential decrease in the atmospheric ^{14}C level, with a half-life of 11 years due to the diffusion of CO_2 into the oceans. By comparing the amount of ^{14}C in a particular cell population with that in the atmosphere the age of the cell population can be determined. The cells in the cortex of the adult human brain have been investigated, and it was found that while non-neuronal cells are replaced, occipital neurons are as old as the individual (Spalding et al., 2005; Bhardwaj et al., 2006). The AMS measurements for these investigations (Palmblad et al., 2005) were performed at the Lawrence Livermore National Laboratory. ^{14}C levels from samples containing as little as 30 μg carbon were analyzed (corresponding to genomic DNA from 15 million cells), thus taking advantage of the full potential of the AMS method.

D. Environmental Studies

A number of radioactive isotopes are distributed throughout the environment as a result of nuclear weapons testing, nuclear fuel reprocessing, nuclear reactor operation, and to a small extent also accidental releases from nuclear facilities. ^{3}H, ^{14}C, ^{99}Tc, ^{129}I, ^{135,134,137}Cs, ^{237}Np, ^{236}U, ^{239,240,241}Pu, and other actinides are all examples of isotopes that can be found in the environment surrounding nuclear facilities. These isotopes can be found in air, water, sediments, aerosol particles, plants, animals, and humans. The most commonly applied analytical tool is β-detection and (for the actinides) α-spectrometry. Applications relevant to human health effects often require significantly higher sensitivity than these two standard methods can provide. AMS has demonstrated improved detection limits for all these isotopes. For example, for plutonium isotopes the reported sensitivity of AMS is $\sim 10^6$ atoms per sample during routine ^{239,240,241,242,244}Pu measurements (Brown et al., 2004). This can be compared with the daily urinary excretion of Pu for one person (in the general population) which is also $\sim 10^6$ atoms.

Fallout of ^{36}Cl from nuclear weapons testing in the 1950s and 1960s has been preserved in glaciers around the world. AMS measurements of this isotope preserved in ice cores have improved estimates of historical, worldwide atmospheric deposition and have allowed the sources of ^{36}Cl in ground water to be better identified (Green et al., 2004). The uranium isotope ^{236}U ($T_{1/2} = 23.4$ million years) is produced by neutron capture in ^{235}U. The ^{236}U/^{238}U ratio increases to 0.1–0.5% in irradiated nuclear fuel. The natural abundance in uranium ore samples is on the order of $\sim 10^{-10}$, giving a very low background from unirradiated material. ^{236}U is therefore a useful tracer of irradiated uranium. An AMS detection limit for ^{236}U/^{238}U of 10^{-8} has been reported (Hotchkis et al., 2000). ^{14}C and ^{129}I have been measured in seawater around radioactive waste dump sites. Half a liter of water is enough to identify traces of these isotopes by AMS (Povinec et al., 2000). The isotope ^{36}Cl has been detected in groundwater samples taken not far from a disposal site for processed nuclear waste in the USA (Cecil et al., 2000). Large amounts of radionuclides are released into the environment in connection with nuclear weapons detonations. All these nuclides can easily be followed in the atmosphere, oceans, and groundwater using AMS. AMS is therefore an important analytical technique in environmental monitoring for nuclear safeguards.

Today's standards for neutron exposure (in the Dosimetry System of 1986 (DS86) and the recently published DS02) are largely dependent on studies of survivors from the Hiroshima and Nagasaki nuclear bombs in August 1945. The radiation effects observed on survivors have to be related to the neutron dose obtained. These doses have until now mostly been obtained by calculations from data regarding the bombs, distances, etc. Another and better means would be to measure the radioisotopes produced *in situ* during the explosion. AMS investigations during the past 10–15 years of the isotopes ^{36}Cl, ^{41}Ca, ^{63}Ni, and others in samples such as concrete, granite, copper, etc. irradiated by the nuclear explosion, as a function of the distance from the hypocenter, have shown the need for revision of the presently adopted dose–response relation for neutrons. The ^{36}Cl/Cl ratio in samples of concrete (Straume et al., 1990) and granite (Nagashima et al., 2004) from Hiroshima has been investigated. ^{41}Ca has been measured in samples of a granite gravestone 107 m from the hypocenter (Rühm et al., 1990). These three investigations all indicate a much "harder" neutron spectrum than has previously been estimated. The radioisotope ^{41}Ca is produced by thermal neutron capture by stable ^{40}Ca. In a recent

investigation tooth samples were collected from exposed survivors as well as from large-distant survivors for comparison. The ^{41}Ca/Ca ratios for the exposed survivors show a significant correlation with distance from the hypocenter (Wallner et al., 2004).

Most investigations up until now have dealt with the thermal neutron spectrum. In a recent investigation the fast neutron spectrum was investigated. The radioisotope ^{63}Ni ($T_{1/2} = 100$ y) is produced in copper by fast neutrons via the nuclear reaction ^{63}Cu(n,p)^{63}Ni. The amount of ^{63}Ni was measured in copper samples taken from the A-bomb Dome in Hiroshima. The results were compared to estimates of the fast neutron fluences from DS86 and DS02 (Rugel et al., 2004).

^{59}Ni is an important radioisotope in nuclear waste management. The isotope is produced by neutron activation, mainly through the nuclear reaction ^{58}Ni(n,γ)^{59}Ni, in the stainless steel close to the core of a nuclear reactor. Three main areas of interest can be identified that require knowledge of the activity concentration of ^{59}Ni.

1. Classification of the construction material in a nuclear power plant on the basis of the activity concentration, in order to be able to define how used parts are to be stored.
2. Refinement of calculation models of the neutron flux in the reactor. This can be done if the content of ^{59}Ni in the different parts of the reactor is known.
3. Classification of operational waste on the basis of its activity concentration, for example, ion exchangers.

The radionuclide ^{59}Ni decays only via electron capture, and the radiation emitted consists primarily of characteristic X-rays. This, in combination with its long half-life of 7.6×10^4 years, makes it difficult to measure by decay counting. PIXEAMS (briefly described in Section IIB.5e) provides an efficient way of measuring ^{59}Ni.

The stable isobar to ^{59}Ni is ^{59}Co. The sample material from the nuclear industry is mainly stainless steel, which contains a certain amount of cobalt. It is therefore necessary to remove the natural cobalt in the sample preparation process. This is done in two steps. The first is dissolution of the stainless steel in HCl followed by the precipitation of nickel with dimethylglyoxime. The second purification step to further reduce the cobalt content utilizes the reaction between nickel and carbon monoxide to form gaseous nickel tetracarbonyl (Ni(CO)$_4$). A number of steel samples obtained from the Swedish nuclear industry have been analyzed using the Lund AMS system. The samples were taken from different positions close to the core, such as the moderator tank, steam separator, guiding rods for the moderator head, and various flanges. The activity found ranged from a few MBq per gram nickel down to a few kBq. Samples of re-circulating water from a PWR reactor have also been analyzed. Activities of the water samples were found to be 10–30 kBq per liter water (Persson et al., 2000a,b; Persson, 2002).

Another example related to the nuclear power industry concerns the release of ^{14}C from power plants, which leads to an increase in the ^{14}C specific activity of the atmosphere and, hence, to an increased radiation exposure of the population. ^{14}C is one of the radionuclides produced to different degrees by neutron-induced reactions in all types of nuclear reactors. It is believed that, of all nuclides released in routine operation by the nuclear power industry, ^{14}C is likely to produce the largest collective dose to the human population. The production of ^{14}C can occur in the fuel, the moderator, the coolant, and the core construction materials, mainly by the reactions:

$$^{17}\mathrm{O}(n,\alpha)^{14}\mathrm{C}$$
$$^{14}\mathrm{N}(n,p)^{14}\mathrm{C}$$

Part of the ^{14}C created in reactors is continuously released as airborne effluents in various chemical forms (CO_2, CO, and hydrocarbons) through the ventilation system of the power plant during normal operation. Only a few liters of air are required using ^{14}C-AMS, compared to 100–1,000 L for decay counting. In a 1-year study, the total airborne ^{14}C effluents from the stack of two light water reactors were measured continuously over 2-week periods (Stenström et al., 1995, 1996a).

The incorporation of ^{14}C into living material, mainly leaves and grass, in the environment of power plants has also been studied. The ^{14}C content in annual tree rings of pine (*Pinus*), located at different distances from power plants has also been measured (Stenström et al., 1996b, 2002b; Hellborg et al., 2000). A detailed investigation concerning ^{14}C levels in terrestrial and fresh water samples from the vicinity of the Ignalina nuclear power plant in Lithuania has been presented in Magnusson et al. (2004, 2007). Approximately 70 samples have been collected, including tree leaves and needles, grass, moss and soil profiles, as well as fresh water plants; covering a distance of up to 32 km from the plant. The investigation showed ^{14}C levels in moss and soil samples taken close to the reactor that were up to 20 times higher than the contemporary background level. The excess ^{14}C could be associated with airborne ^{14}C particulates released from the plant.

The nuclear fuel reprocessing facility at Sellafield in northwest England is known to release substantial amounts of ^{14}C. In Figure 11 the ^{14}C content in grass samples collected in September 1996 at various distances from the Sellafield plant is presented (Hellborg et al., 2000). The highest activity, found at the sample site closest to the facility, was 447 ± 9 Bq/kgC (Bq per kg of carbon). This is approximately 80% above the natural level, found at distances >8–9 km from the facility.

The effective dose to the population has been calculated from measured values of the excess of ^{14}C specific activity at different types of nuclear facilities (Stenström, 2002a). The commonly applied assumption in ^{14}C dosimetry, that ^{14}C in the human body is in equilibrium with that in the environment, was used. In Table 6, taken from Stenström et al. (2002b), the excess ^{14}C specific activity and the effective dose rate (μSv per year) to the most exposed individual is given. The most exposed individual is a person living within 3 km of the site of the release. The absorbed dose (mGy) to fat and bone marrow can be 2–3 times higher than the effective dose (μSv).

V. CONCLUSIONS AND FUTURE PERSPECTIVES

Accelerator mass spectrometry (AMS) is a vital field with an increasing number of applications. Its vitality is demonstrated in

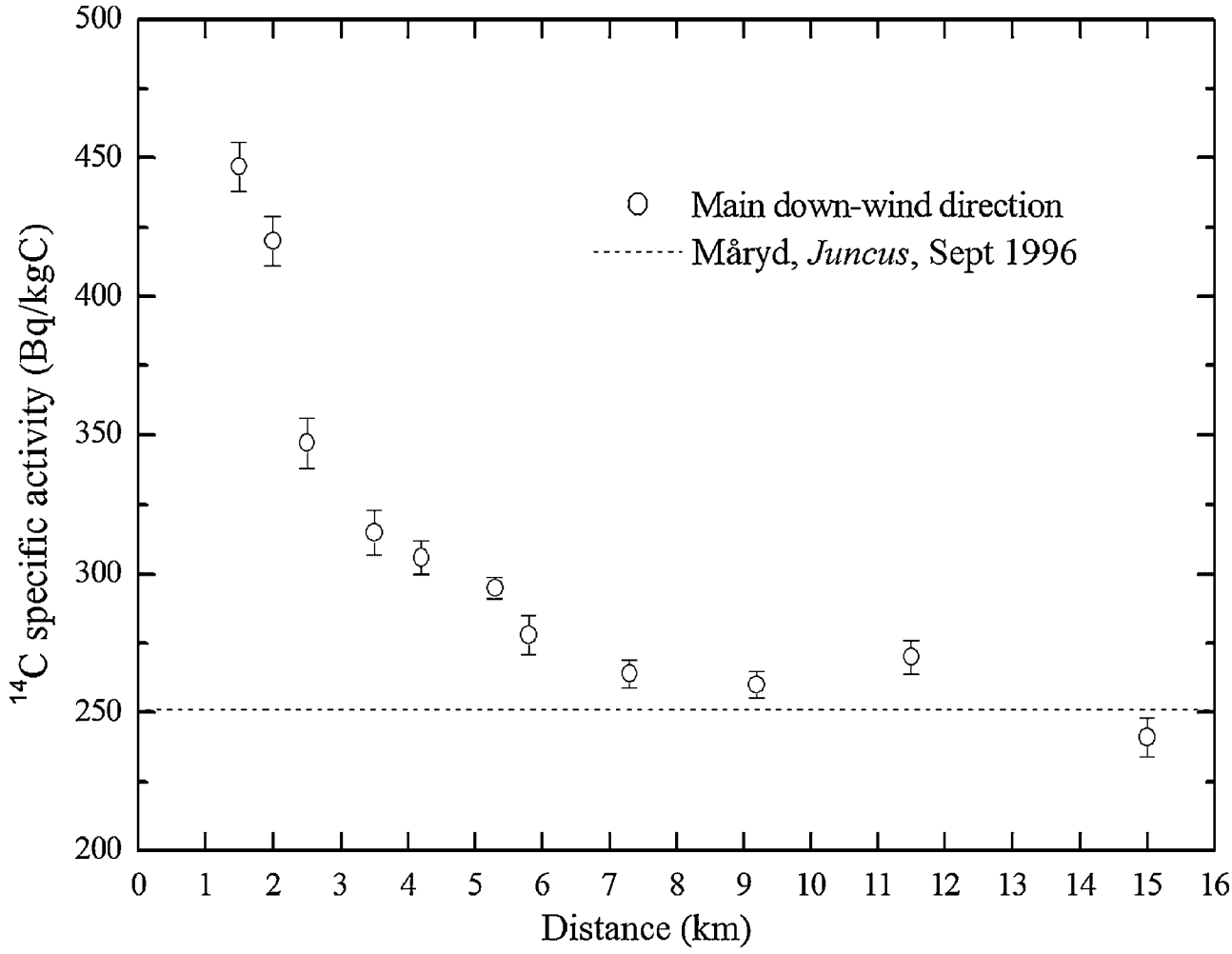

FIGURE 11. The ^{14}C specific activity in grass collected at various distances in the NNE direction from the Thorp (Thermal Oxide Reprocessing Plant) at the Sellafield nuclear fuel reprocessing facility. Måryd is a "clean air" site 10 km east of Lund.

TABLE 6. Local excess ^{14}C specific activity due to releases from various nuclear installations and the related effective dose to the most exposed individual

Site	Excess ^{14}C specific activity (Bq/kgC)	Effective dose rate (μSv/y)
Barsebäck, Sweden	2–4	0.1–0.2
Forsmark, Sweden	6–30	0.3–1.7
Sellafield, UK	200	11
Pickering, Canada	4600	300
Cernavoda, Romania	60	3.3
Natural levels	226	12

the number of new dedicated facilities installed during recent years. Some of these newly installed accelerators are used by private companies for biomedical applications. During the 30 years since the introduction of AMS it has evolved from the academic world of nuclear physics to the commercial world.

The sophistication of the applications of AMS and the range of applications has been increasing for several years and it appears that it will continue, at least, in the near future. The developments are the result of improvements in the technique itself, and the use of new AMS isotopes.

Accelerator mass spectrometry (AMS) is playing an increasing role in archeology as well as the geosciences. The considerable reduction in sample size, compared to the decay-counting technique, has led to new applications. The introduction of gas ion sources will further reduce the size of samples needed for radiocarbon dating, and the dating of samples as small as 10 μg carbon now seems possible. Surface exposure dating and *in situ* cosmogenic dating are already an important application of AMS and their rapid expansion is foreseen.

As a result of the investigations performed during the past 10 years, new types of instruments have become available. Compact accelerators running at voltages as low as 200 kV for radiocarbon dating and biomedical applications are already commercially available. The use of lower voltages and simpler technology has already led to an increase in the number of laboratories that perform AMS, and this expansion will certainly continue. With some modifications and extensions the sub-MV accelerators should be able to measure many of the relevant isotopes, such as ^{10}Be, ^{26}Al, ^{41}Ca, ^{129}I, ^{236}U, and the Pu isotopes with acceptable sensitivity. Another important improvement during recent years is the interfacing of standard analytical instruments such as gas chromatographs and high-pressure liquid chromatographs with a gas-fed, negative ion source. This allows AMS to be used for real-time analysis. It is important that the interface provides efficient conversion of a wide variety of biological molecules for the ion source.

As smaller accelerators are installed in new laboratories, the existing larger facilities will be used to analyze isotopes with severe interference from isobars, or for the development of as yet unexplored isotopes. Isotopes that appear to be impossible to measure at low isotope ratios with sub-MV accelerators include ^{32}Si, ^{53}Mn, ^{59}Ni, ^{60}Fe, and ^{99}Tc.

A promising development in the application of other types of accelerators is the use of a mini-cyclotron, recently demonstrated to be reliable for ^{14}C measurements. When the isotopes being studied are rare gases, a cyclotron, a single-stage electrostatic accelerator or a linear accelerator may be used. Investigations of ^{39}Ar and ^{81}Kr have also been performed with a superconducting linear accelerator.

ACKNOWLEDGMENTS

A number of people have contributed in different ways during the preparation of this article. We are especially grateful to Dr. Sergei Bazhal, Dr. Dag Brune, Dr. Mikko Faarinen, Professor Klas Malmqvist, Dr. Greg Norton, Professor Walter Kutschera, Mrs. Pia Sköld, Dr. Kristina Stenström, Mr. Max Strandberg, and Professor Harry Whitlow.

REFERENCES

Alley RB, Marotzke J, Nordhaus WD, Overpeck JT, Peteet DM, Pielke RA, Pierrehumbert RT, Rhines PB, Stocker TF, Talley LD, Wallace JM. 2003. Abrupt climate change. Science 299(5615):2005–2010.

Alvarez LW, Cornog R. 1939. ^{3}He in helium. Phys Rev 56:379.

Andrée M, Oeschger H, Siegenthaler U, Riesen T, Moell M, Amman B, Tobolski K. 1986. ^{14}C dating of plant macrofossils in lake sediment. Radiocarbon 28(2A):411–416.

Balter M. 2006. Mild climate, lack of moderns let last Neanderthals linger in Gibraltar. Science 313:1557.

Bard E, Raisbeck GM, Yiou F, Jouzel J. 1997. Solar modulation of cosmogenic nuclide production over the last millenium: Comparison between ^{14}C and ^{10}Be records. Earth Planetary Sci Lett 150(3–4):453–462.

Barnekow L, Possnert G, Sandgren P. 1998. AMS ^{14}C chronologies of Holocene lake sediments in the Abisko area, northern Sweden—A comparison between dated bulk sediment and macrofossil samples. Geologiska Föreningens i Stockholm Förhandlingar 120:59–67.

Becker B, Kromer B. 1986. Extension of the Holocene dendrochronology by the Preboreal pine series 8800–10100 BP. Radiocarbon 28(2B):961–967.

Beer J, Baumgartner S, Hannen-Dittrich B, Hauenstein J, Kubik P, Lukasczyk C, Mende W, Stellmacher R, Suter M. 1994. Solar variability traced by cosmogenic isotopes. In: Pap JM, Fröhlich C, Hudson HS, Solanki SK, editors. The sun as a variable star: Solar and stellar irradiance variations. Cambridge: Cambridge University Press. pp 291–300.

Beer J, Mende W, Stellmacher R. 2000. The role of the sun in climate forcing. Quaternary Sci Rev 19(1):403–415.

Bennett CL, Beukens RP, Clover MR, Gove HE, Liebert RB, Litherland AE, Purser KH, Sondheim WE. 1977. Radiocarbon dating using electrostatic accelerators. Science 198:508–510.

Beukens RP, Lee HW. 1981. The production of small carbon samples by r.f. dissociation of acetylene. Proc. Symposium on AMS, Argonne, pp 416–425.

Bhardwaj RR, Curtis MA, Spalding KL, Buchholz BA, Fink D, Bjork-Eriksson T, Nordborg C, Gage FH, Druid H, Eriksson PS, Frisén J. 2006. Neocortical neorogenesis in humans is restricted to development. Proc Natl Acad Sci 103:12564–12568.

Biddulph DL. 2004. PhD Thesis, University of Arizona.

Bonani G, Balzer R, Hofman HJ, Morenzoni E, Nessi M, Suter M, Wölfli W. 1984. Properties of milligram size samples prepared for AMS ^{14}C dating at ETH. Nucl Instrum Method B 5(2):284–288.

Bonani G, Ivy S, Wölfli W, Broshi M, Carmi I, Strugnell J. 1992. Radiocarbon dating of fourteen Dead Sea scrolls. Radiocarbon 34(3):843–849.

Bonani G, Ivy S, Hajdas I, Niklaus TR, Suter M. 1994. AMS ^{14}C age determinations of tissue, bone and grass samples from the Ötztal Ice Man. Radiocarbon 36(2):247–250.

Bond G, Kromer B, Beer J, Muscheler R, Evans MN, Showers W, Hoffmann S, Lotti-Bond R, Hajdas I, Bonani G. 2001. Persistent solar influence on North Atlantic climate during the Holocene. Science 294:2130–2136.

Broecker WS. 1991. The great ocean conveyor. Oceanography 4(2):79–89.

Broecker WS. 1997. Thermohaline circulation, the Achilles Heel of our climate system: Will man-made CO_2 upset the current balance? Science 278(5343):1582–1588.

Broecker WS. 1998. Paleocean circulation during the last deglaciation: A bipolar seesaw? Paleoceanography 13(2):119–121.

Broecker WS. 2003. Does the trigger for abrupt climate change reside in the ocean or in the atmosphere. Science 300(5625):1519–1522.

Bronk Ramsey C, Hedges REM. 1990. A gaseous ion source for routine AMS radiocarbon dating. Nucl Instrum Methods B 52:322–326.

Bronk Ramsey C, Higham T, Bowles A, Hedges R. 2004. Improvements to the pre-treatment of bone at Oxford. Radiocarbon 46(1):155–163.

Brown TA, Nelson DE, Mathewes W, Vogel JS, Southon JR. 1989. Radiocarbon dating of pollen by accelerator mass spectrometry. Quaternary Res 32:205–212.

Brown TA, Marchetti AA, Martinelli RE, Cox CC, Knezovich JP, Hamilton TF. 2004. Actinide measurements by accelerator mass spectrometry at Lawrence Livermore National Laboratory. Nucl Instrum Methods B 223/224:788–795.

Brune D, Hellborg R, Whitlow HJ, Hunderi O. 1997. Surface characterization. Weinheim: Wiley-VCH. 702 p.

Cecil LD, Welhan JA, Green JR, Grape SH, Sudicky ER. 2000. Use of chlorine-36 to determine regional-scale aquifer dispersivity, eastern Snake River Plain aquifer, Idaho/USA. Nucl Instrum Methods B 172:679–687.

Chen M, Li D, Xu S, Chen G, Shen L, Lu X, Zhang W, Zhang Y, Zhong Z, Zhang Y. 1995. Breakthrough of the Mini-Cyclotron Mass Spectrometer for ^{14}C Analysis. Radiocarbon 37:675–681.

Chen M, Lu X, Li D, Liu Y, Zhou W, Chen G, Shen L, Xu S, Zhang Y. 2000. Minicyclotron (SMCAMS)-based accelerator mass spectrometry and real ^{14}C measurements. Nucl Instrum Methods B 172:193–200.

Collon P, Kutschera W, Antaya T, Davids B, Fauerbach M, Harkewicz R, Hellstrom M, Morrissey D, Sherrill B, Steiner M, Pardo R, Paul M. 1997. Measurement of ^{81}Kr in the atmosphere. Nucl Instrum Methods B 123:122–127.

Collon P, Bichler M, Caggiano J, DeWayne Cecil L, El Masri Y, Golser R, Jiang CL, Heinz A, Hendersen D, Kutschera W, Lehmann BE, Leleux P, Loosli HH, Pardo RC, Paul M, Rehm KE, Schlosser P, Scott RH, Smethie WM, Jr., Vondrasek R. 2004. Development of an AMS method to study oceanic circulation characteristics using cosmogenic 39Ar. Nucl Instrum Methods B 223/224:428–434.

Czernik J, Goslar T. 2001. Preparation of graphite targets in the Gliwice radiocarbon laboratory for AMS ^{14}C dating. Radiocarbon 43(2A):283–291.

Damon PE, Donahue DJ, Gore BH, Hatheway AL, Jull AJT, Linick TW, Sercel PJ, Toolin LJ, Bronk CR, Hall ET, Hedges REM, Housley R, Law IA, Perry C, Bonani G, Trumbore S, Woelfli W, Ambers JC, Bowman SGE, Leese MN, Tite MS. 1989. Radiocarbon dating of the shroud of turin. Nature 337(6208):611–615.

Dansgaard W, Johnsen SJ, Clausen HB, Dahl-Jensen D, Gundestrup NS, Hammer CU, Hvidberg CS, Steffensen JP, Sveinbjornsdottir AE, Jouzel J, Bond G. 1993. Evidence for general instability of past climate from a 250-kyr ice-core record. Nature 364(6434):218–220.

Ertunç T, Xu S, Bryant CL, Maden C, Murray C, Currie M, Freeman SPHT. 2005. Progress in target production of sub-milligram samples at the Nerc Radiocarbon Laboratory. Radiocarbon 47(3):453–464.

Faarinen M, Magnusson CE, Hellborg R, Mattsson S, Kiisk M, Persson P, Schütz A. 2001. ^{26}Al investigations at the AMS-laboratory in Lund. J Inorg Biochem 87:57–61.

Fairbanks RG, Mortlock RA, Chiu TC, Cao L, Kaplan A, Guilderson TP, Fairbanks TW, Bloom AL, Grootes PM, Nadeau MJ. 2005. Radiocarbon calibration curve spanning 0 to 50000 years BP based on paired ^{230}Th/^{234}U/^{238}U and ^{14}C dates on pristine corals. Quaternary Sci Rev 24:1781–1796.

Fifield LK, Synal HA, Suter M. 2004. Accelerator mass spectrometry of plutonium at 300 kV. Nucl Instrum Methods B 223/224:802–806.

Friedrich M, Remmele S, Kromer B, Hofmann J, Spurk M, Klaus FK, Orcel C, Küppers M. 2004. The 12,460-Year Hohenheim Oak and Pine Tree-Ring Chronology from Central Europe—A Unique Annual Record for Radiocarbon Calibration and Paleoenvironment Reconstructions. Radiocarbon 46:1111–1122.

Goodsite ME, Rom W, Heinemeier J, Lange T, Ooi S, Appleby PG, Shotyk W, van der Knaap WO, Lohse C, Hansen TS. 2001. High resolution AMS 14C dating of post-bomb peat archives of atmospheric pollutants. Radiocarbon 43(2B):495–515.

Gosse JC, Phillips FM. 2001. Terrestrial in situ cosmogenic nuclides: Theory and application. Quaternary Sci Rev 20:1475–1560.

Gracjar M, Döbeli M, Kubik PW, Maden C, Suter M, Synal HA. 2004. ^{10}Be measurements with terminal voltages below 1 MV. Nucl Instrum Methods B 223/224:190–194.

Green JR, Cecil LD, Synal HA, Santos J, Kreutz KJ, Wake CP. 2004. A high resolution record of chlorine-36 nuclear-weapons-tests fallout from Central Asia. Nucl Instrum Methods B 223/224:854–857.

Grootes PM, Stuiver M, Farwell GW, Schaad TP, Schmidt FH. 1980. Enrichment of ^{14}C and sample preparation for beta and ion counting. Radiocarbon 22(2):487–500.

Gunnarsson M, Mattsson S, Stenström K, Leide-Svegborn S, Erlandsson B, Faarinen M, Hellborg R, Kiisk M, Nilsson L-E, Nosslin B, Persson P, Skog G, Åberg M. 2000. AMS studies of the long-term turnover of ^{14}C-labelled fat in man. Nucl Instrum Methods B 172:939–943.

Gunnarsson M. 2002a. Biokinetics and radiation dosimetry of ^{14}C-labelled triolein, urea, glycocholic acid and xylose in man. (Ph.D. Thesis) University of Lund, Lund, Sweden.

Gunnarsson M, Leide-Svegborn S, Stenström K, Skog G, Nilsson L-E, Hellborg R, Mattsson S. 2002b. No radiation protection reasons for restrictions on ^{14}C urea breath tests in children. Br J Radiol 75:982–986.

Gunnarsson M, Stenström K, Leide-Svegborn S, Faarinen M, Magnusson CE, Åberg M, Skog G, Hellborg R, Mattsson S. 2003. Biokinetics and radiation dosimetry for patients undergoing a glycerol tri[1-^{14}C]oleate fat malabsorption breath test. Appl Radiat Isot 58:517–526.

Guo Z, Liu K, Yan X, Xie Y, Fang J, Chen J. 2007. Feasibility studies of RFQ based ^{14}C accelerator mass spectrometry. In proceedings of the 10th International Conference on Accelerator Mass Spectrometry, Berkeley, CA (2005). Nucl Instrum Methods B 259:204–207.

Hedges REM, van Klinken GJ. 1992. A review of current approaches in the pretreatment of bone for radiocarbon dating by AMS. Radiocarbon 34(3):279–291.

Hellborg R, Erlandsson B, Faarinen M, Håkansson H, Håkansson K, Kiisk M, Magnusson CE, Persson P, Skog G, Stenström K, Mattsson S, Thornberg C. 2000. Environmental radiation protection studies related to nuclear industries, using AMS, Vol. 576. American Institute of Physics: Appl of Accelerators in Research and Industry. pp 377–381.

Hellborg R. 2005. Electrostatic accelerators. Heidelberg: Springer. 620 p.

Hotchkis MAC, Child D, Fink D, Jacobsen GE, Lee PJ, Mimo N, Smith AM, Tuniz C. 2000. Measurement of 236U in environmental media. Nucl Instrum Methods B 172:659–665.

Houghton JT, Ding Y, Griggs DJ, Noguer M, van der Linden PJ, Xiaosu D. 2001. Climate Change 2001—The Scientific Basis: Contribution of Working Group I to the Third Assessment Report of the Intergovernmental Panel on Climate Change. Cambridge: Cambridge University Press. p 944.

Hughen K, Lehman S, Southon J, Overpeck J, Marchal O, Herring C, Turnbull J. 2004. ^{14}C activity and global carbon cycle changes over the past 50000 years. Science 303:202–207.

Hughey BJ, Skipper PL, Klinkowstein RE, Shefer RE, Wishnok JS, Tannenbaum SR. 2000. Low-energy biomedical GC-AMS system for ^{14}C and ^{3}H detection. Nucl Instrum Methods B 172:40–46.

Hut G, Östlund HG, van der Borg K. 1986. Fast and complete CO_2-to-graphite conversion for ^{14}C accelerator mass spectrometry. Radiocarbon 28(2A):186–190.

Jacobi RM, Higham TFG, Bronk Ramsey C. 2006. AMS radiocarbon dating of Middle and Upper Palaeolithic bone in the British Isles: Improved reliability using ultrafiltration. J Quaternary Sci 21(5):557–573.

Jahns S. 2000. Late-glacial and Holocene woodland dynamics and land-use history of the Lower Oder valley, north-eastern Germany, based on two, AMS ^{14}C-dated, pollen profiles. Veget Hist Archaeobot 9:111–123.

Jiang S, He M, Dong K, Yue D, Wu S, Xu G, Qin J, You Q, Zheng Y, Guan Y, Liang Q, Zhang G, Zhao X, Wang Q, Liu S. 2004. The measurement of ^{41}Ca and its application for the cellular Ca^{2+} concentration fluctuation caused by carcinogenic substances. Nucl Instrum Methods B 223/224:750–753.

Johansson SAE, Campbell JL, Malmqvist KG. 1995. PIXE—A novel technique for elemental analysis. New York: John Wiley & Sons.

Johansson TB, Akselsson KR, Johansson SAE. 1970. X-ray analysis: Elemental trace analysis at the 10^{-12}g level. Nucl Instrum Methods 84:141–143.

Key RM, Quay PD, Schlosser P, McNichol A, Reden KF, Schneider BJ, Elder KL, Stuiver M, Ostlund HG. 2002. WOCE Radiocarbon IV: Pacific Ocean results; P10, P13N, P14C, P18, P19, & S4P. Radiocarbon 44(1):239–392.

Kilian MR, van der Plicht J, van Geel B, Goslar T. 2002. Problematic ^{14}C-AMS dates of pollen concentrates from Lake Gosciaz (Poland). Quaternary Int 88:21–26.

Kilius LR, Rucklidge JC, Litherland AE. 1987. Accelerator mass spectrometry of ^{129}I at Isotrace. Nucl Instrum Methods B 223/224:72–76.

Klein M, Mous D, Gottdang A. 2006. A compact 1MV multi-element AMS system. Nucl Instrum Methods B 249:764–767.

Klody GM, Schroeder JB, Norton GA, Loger RL, Kitchen RL, Sundqvist ML. 2004. New results for single stage low energy carbon AMS. Presented at the 8th European Conference on Accelerators in Applied Research and Technology (ECAART8).

Kutschera W. 2005. Progress in isotope analysis at ultra-trace level by AMS. Int J Mass Spectrom 242:145–160.

Lanting JN, Aerts-Bijma AT, van der Plicht J. 2001. Dating of cremated bones. Radiocarbon 43(2A):249–254.

Lee HW, Galindo-Uribarri A, Chang KH, Kilius LR, Litherland AE. 1984. The $^{12}CH_2^{2+}$ molecule and radiocarbon dating by accelerator mass spectrometry. Nucl Instrum Methods B 5:208–210.

Leide-Svegborn S, Stenström K, Olofsson M, Mattsson S, Nilsson LE, Nosslin B, Pau K, Johansson L, Erlandsson B, Hellborg R, Skog G. 1999. Biokinetic and radiation doses for carbon-14 urea in adults and children undergoing the Helicobacter pylori breath test. Eur J Nucl Med 26:573–580.

Liu Y, Wang S, Li D, Chen G, Jia W, Chen M. 2007. The status of SMCAMS after recent upgrades. In proceedings of the 10th International Conference on Accelerator Mass Spectrometry, Berkeley, CA. Nucl Instrum Methods B 259:62–65.

Long A, Davis OK, DeLanois J. 1992. Separation and ^{14}C dating of pure pollen from lake sediments: Nanofossil AMS dating. Radiocarbon 34(3):557–560.

Lopez-Guitérrez JM, Synal HA, Suter M, Schnabel C, García-Leon M. 2000. Accelerator mass spectrometry as a powerful tool for the determination of ^{129}I in rainwater. Appl Radiat Isot 53:81–85.

Lowe DC, Judd WJ. 1987. Graphite target preparation for radiocarbon dating by accelerator mass spectrometry. Nucl Instrum Methods B 28(1):113–116.

Magnusson Å, Stenström K, Skog G, Adliene D, Adlys G, Hellborg R, Olariu A, Zakaria M, Rääf C, Mattsson S. 2004. Levels of ^{14}C in the terrestrial environment in the vicinity of two European nuclear power plants. Radiocarbon 46:863–868.

Magnusson Å, Stenström K, Adliene D, Adlys G, Dias C, Rääf C, Skog G, Zakaria M, Mattsson S. 2007. Carbon-14 levels in the vicinity of the Lithuanian nuclear power plant Ignalina. In proceedings of the 10th International Conference on Accelerator Mass Spectrometry, Berkeley, CA. Nucl Instrum Methods B 259:530–535.

Manning MP, Reid RC. 1977. C-H-O systems in the presence of an iron catalyst. Ind Eng Chem Process Des Dev 16(3):358–361.

Matsumoto K, Key RM. 2004. Natural radiocarbon distribution in the Deep Ocean. In: Shiyomi M, Kawahata H, Koizumi H, Tsuda A, Awaya Y, editors. Global environmental change in the ocean and on land. Tokyo: TERRAPUB. pp 45–58.

Mattsson S, Gunnarsson M, Leide-Svegborn S, Nosslin B, Nilsson L-E, Thorsson O, Valind S, Åberg M, Östberg H, Hellborg R, Stenström K, Erlandsson B, Faarinen M, Kiisk M, Magnusson CE, Persson P, Skog G. 2001. Biokinetic and dosimetric investigations of ^{14}C-labeled substances in man using AMS, Vol. 576. Mel Ville, New York: Appl of Accelerators in Research and Industry (AIP Conf Proc). pp 394–398.

Mellars P. 2006. A new radiocarbon revolution and the dispersal of modern humans in Eurasia. Nature 439:931–935.

Middleton R, Adams CT. 1974. A close to universal negative ion source. Nucl Instrum Methods 118:329–336.

Muller RA. 1977. Radioisotope dating with a cyclotron. Science 196(4289): 489–494.

Nagashima Y, Seki R, Matsuhiro T, Takahashi T, Sasa K, Sueki K, Hoshi M, Fujita S, Shizuma K, Hasai H. 2004. Chlorine-36 in granite samples from the Hiroshima A-bomb site. Nucl Instrum Methods B 223/224: 782–787.

Nelson DE, Korteling RG, Stott WR. 1977. Carbon-14: Direct detection at natural concentrations. Science 198:507–508.

Ognibene TJ, Bench G, Brown TA, Vogel JS. 2004. The LLNL accelerator mass spectrometry system for biochemical ^{14}C-measurements. Nucl Instrum Methods B 223/224:12–15.

Ognibene TJ, Bench G, Vogel JS. 2003. A high-throughput method for the conversion of CO_2 obtained from biochemical samples to graphite in septa-sealed vials for quantification of ^{14}C via accelerator mass spectrometry. Anal Chem 75(9):2192–2196.

Olsson I. 1986. Radiometric dating. In: Handbook of Palaeoecology and Palaeohydrology. Chichester, UK: John Wiley & Sons Ltd. pp 273–312.

Palmblad M, Bruce A, Buchholz A, Hillegonds DJ, Vogel JS. 2005. Neoroscience and accelerator mass spectrometry. J Mass Spectrom 40:154–159.

Paul M. 1990. Separation of isobars with a gas-filled magnet. Nucl Instrum Methods B 52:315–321.

Pearson GW, Becker B, Qua F. 1993. High-precision ^{14}C measurement of German and Irish oaks to show the natural ^{14}C variations from 7890 to 5000 BC. Radiocarbon 35(1):93–104.

Persson J. 1997. Development of a sample preparation procedure for the production of elemental carbon from urine for AMS analyses. Results from long-term studies after a ^{14}C-urea breath test. Report 02/97 LUNFD6/(NFFR-5010)/1-40 Lund.

Persson P, Erlandsson B, Freimann K, Hellborg R, Larsson R, Persson J, Skog G, Stenström K. 2000a. Determination of the detection limit of ^{59}Ni at the Lund AMS facility by using characteristic projectile X-rays. Nucl Instrum Methods B 160:510–514.

Persson P, Kiisk M, Erlandsson B, Faarinen M, Hellborg R, Skog G, Stenström K. 2000b. Detection of ^{59}Ni at the Lund AMS facility. Nucl Instrum Methods B 172:188–192.

Persson P. 2002. Improved detection limit for ^{59}Ni using the technique of accelerator mass spectrometry. (PhD Thesis) Lund University, Lund, Sweden.

Pilcher JR, Baillie MGL, Schmidt B, Becker B. 1984. A 7272-year tree-ring chronology for western Europe. Nature 312:150–152.

van der Plicht J, Beck JW, Bard E, Baillie MGL, Blackwell PG, Buck CE, Friedrich M, Guilderson TP, Hughen KA, Kromer B, McCormac FG, Bronk Ramsey C, Reimer PJ, Reimer RW, Remmele S, Richards DA, Southon JR, Stuiver M, Weyhenmeyer CE. 2004. NotCal04—Comparison/Calibration ^{14}C Records 26-50Cal Kyr BP. Radiocarbon 46(3):1225–1238.

Povinec PP, Oregioni B, Jull AJT, Kieser WE, Zhao XL. 2000. AMS measurements of ^{14}C and ^{129}I in seawater around radioactive waste dump sites. Nucl Instrum Methods B 172:672–678.

Povinec PP, LaRosa JJ, Lee SH, Mulsow S, Osvath I, Wyse E. 2001. Recent developments in radiometric and mass spectrometry methods for marine radioactivity measurements. J Radioanal Nucl Chem 248:713–718.

Purser KH, Liebert RB, Litherland AE, Benkens RP, Gove HE, Bennett CL, Clover MR, Sondheim WE. 1977. An attempt to detect stable N^- ions from a sputter ion source and some implications of the results for the design of tandems for ultra-sensitive carbon analysis. Rev Phys Appl 12:1487–1492.

Purser KH, Liebert RB, Russo CJ. 1980. MACS: An accelerator-based radioisotope measuring system. Radiocarbon 22:794–806.

Purser KH, Smick TH, Purser RK. 1990. A precision ^{14}C accelerator mass spectrometer. Nucl Instrum Methods B 52:263–268.

Raisbeck GM, Yiou F, Fruneau M, Loiseaux JM. 1978. Beryllium-10 mass spectrometry with a cyclotron. Science 202(4364):215–217.

Raisbeck GM, Yiou F, Fruneau M, Loiseaux JM, Lieuvin M, Ravel JC, Lorius C. 1981. Cosmogenic ^{10}Be concentrations in Antarctic ice during the past 30,000 years. Nature 292(5826):825–826.

Raisbeck GM, Yiou F, Cattani O, Jouzel J. 2006. ^{10}Be evidence for the Matuyama-Brunhes geomagnetic reversal in the EPICA dome C ice core. Nature 444(7115):82–84.

Ramsey CCB, Ditchfield P, Humm M. 2004. Using a gas ion source for radiocarbon AMS and GC-AMS. Radiocarbon 46(1):25–32.

Regnell J. 1992. Preparing pollen concentrates for AMS dating: A methodological study from a hard-water lake in southern Sweden. Boreas 21(4):373–377.

Reimer PJ, Baillie MGL, Bard E, Bayliss A, Beck JW, Bertrand CJH, Blackwell PG, Buck CE, Burr GS, Cutler KB, Damon PE, Edwards RL, Fairbanks RG, Friedrich M, Guilderson TP, Hogg AG, Hughen KA, Kromer B, Gerry M, Sturt Ramsey CB, Reimer RW, Remmele S, Southon JR, Stuiver M, Talamo S, Taylor FW, van der Plicht J, Weyhenmeyer CE. 2004. IntCal04 terrestrial radiocarbon age calibration, 0-26Cal Kyr BP. Radiocarbon 46(3):1029–1058.

Rugel G, AraZi A, Carroll KL, Faestermann T, Knie K, Korschinek G, Marchetti AA, Martinelli RE, McAninch JE, Rühm W, Straume T, Wallner A, Wallner C. 2004. Low-level measurement of ^{63}Ni by means of accelerator mass spectrometry. Nucl Instrum Methods B 223/224: 776–781.

Rühm W, Kato K, Korschinek G, Morinaga H, Urban A, Zerle L, Nolte E. 1990. The neutron spectrum of the Hiroshima A-bomb and the dosimetry system 1986. Nucl Instrum Methods B 52:557–562.

Rühm W, Carroll KL, Egbert SD, Faestermann T, Knie K, Korschinick G, Martinelli RE, Marchetti AA, McAninch JE, Rugel G, Straume Y, Wallner A, Wallner C, Fujita S, Hasai H, Hoshi M, Shizuma K. 2007. Neutron-induced 63Ni in copper samples from Hiroshima and Nagasaki: a comprehensive presentation of results obtained at the Munich Maier-Leibnitz Laboratory. Radiat Environ Biophys 46:327–338.

Santos GM, Southon JR, Druffel-Rodriguez KC, Griffin S, Mazon M. 2004. Magnesium perchlorate as an alternative water trap in AMS graphite sample preparation: A report on sample preparation at KCCAMS at the University of California, Irvine. Radiocarbon 46(1):165–173.

Schneider RJ, Kim SW, von Reden KF, Hayes JM, Wills JSC, Griffin VS, Session AL, Sylva S. 2004. A gas ion source for continuous-flow AMS. Nucl Instrum Methods B 223/224:149–154.

Schroeder JB, Hauser TM, Klody GM, Norton GA. 2004. Initial results with low energy single stage AMS. Radiocarbon 46(1):1–4.

Sharma M. 2002. Variations in solar magnetic activity during the last 200 000 years: Is there a Sun-climate connection? Earth Planetary Sci Lett 199:459–472.

Skipper PL, Hughey BJ, Liberman RG, Choi MH, Wishnok JS, Klinkowstein RE, Shefer RE, Tannen baum SR. 2004. Bringing AMS into the bioanalytical chemistry lab. Nucl Instrum Methods B 223/224:740–744.

Skog G. 2002. Accelerator mass spectrometry in quaternary geology and archaeology. In: Olariu A, Stenström K, Hellborg R, editors. Proc Int Conf Applications of High Precision Atomic and Nuclear Methods. Bucharest, Romania: Editura Academiei Romane. pp 232–242.

Skog G. 2007. The single stage AMS machine at Lund University: Status report. In proceedings of the 10th International Conference on Accelerator Mass Spectrometry, Berkeley, CA. Nucl Instrum Methods B 259:1–6.

Spalding KL, Bhardwaj RR, Buchholz BA, Druid H, Frisén J. 2005. Retrospective birth dating of cells in humans. Cell 122:133–143.

Spurk M, Friedrich M, Hofmann J, Remmele S, Frenzel B, Leuschner HH, Kromer B. 1998. Revisions and extensions of the Hohenheim oak and pine chronologies: New evidence about the timing of the Younger Dryas/preboreal transition. Radiocarbon 40(3):1107–1116.

Steier P, Golser R, Liechtenstein V, Kutschera W, Priller A, Vockenhuber C, Wallner A. 2005. Opportunities and limits of AMS with 3 MV tandem accelerators. Nucl Instrum Methods B 240:445–451.

Stenström K, Erlandsson B, Hellborg R, Wiebert A, Skog G, Vesanen R, Alpsten M, Bjurman B. 1995. A one-year study of the total air-borne ^{14}C effluents from two Swedish light-water reactors, one boiling water- and one pressurized water reactor. J Radioanal Nucl Chem 198:203–213.

Stenström K, Erlandsson B, Hellborg R, Wiebert A, Skog G. 1996a. Determination of the $^{14}CO_2$ and the total airborne ^{14}C releases from two Swedish light-water reactors using accelerator mass spectrometry. Radioactivity Radiochem 7:32–36.

Stenström K, Erlandsson B, Hellborg R, Wiebert A, Skog G. 1996b. Environmental levels of carbon-14 around a Swedish nuclear power plant measured with accelerator mass spectrometry. Nucl Instrum Methods B 113:474–476.

Stenström K, Leide-Svegborn S, Erlandsson B, Hellborg R, Mattsson S, Nilsson L-E, Nosslin B, Skog G, Wiebert A. 1996c. Application of Accelerator Mass Spectrometry (AMS) for high-sensitivity measurements of $^{14}CO_2$ in long-term studies of fat metabolism. Appl Radiat Isot 47:417–422.

Stenström K, Leide-Svegborn S, Erlandsson B, Hellborg R, Skog G, Mattsson S, Nilsson L-E, Nosslin B. 1997. A programme for long-term retension studies of ^{14}C-labelled compounds in man using the Lund AMS facility. Nucl Instrum Methods B 123:245–248.

Stenström K. 2002a. Accelerator Mass Spectrometry—An Introductory Overview. In: R. Hellborg (Ed.), Symposium of North Eastern Accelerator Personnel, Lund, Sweden, 22–25 October, 2001, SNEAP XXXIV, (2001) pp 48–60.

Stenström K, Erlandsson B, Faarinen M, Hellborg R, Kiisk M, Persson P, Skog G, Thornberg C, Mattsson S, Olariu A, Olariu S, Baciu F, Cutoiu D. 2002b. Radioecological applications of ^{14}C measurements at the Lund accelerator mass spectrometry (AMS) facility. In: Olariu A, Stenström K, Hellborg R, editors. Proceedings of Applications of high precision atomic & nuclear methods. Bucarest: Academiei Romane. pp 254–265.

Straume T, Finkel RC, Eddy D, Kubik PW, Gove HE, Sharma P, Fujita S, Hoshi M. 1990. Use of accelerator mass spectrometry in the dosimetry of Hiroshima neutrons. Nucl Instrum Methods B 52:552–556.

Stuiver M. 1982. A high-precision calibration of the AD radiocarbon time scale. Radiocarbon 24(1):1–26.

Suter M, Jacob S, Synal HA. 1997. AMS of ^{14}C at low energies. Nucl Instrum Methods B 123:148–152.

Suter M, Huber R, Jacob S, Schroeder JB, Synal HA. 1999. AIP conference proceedings 475, Applications of Accelerators in Research & Industry 2: 665.

Suter M, Jacob SWA, Synal HA. 2000. Tandem AMS at sub-MeV energies—Status and prospects. Nucl Instrum Methods B 172:144–151.

Synal HA, Jacob S, Suter M. 2000. The PSI/ETH small radiocarbon dating system. Nucl Instrum Methods B 172:1–7.

Synal HA, Döbeli M, Jacob S, Stocker M, Suter M. 2004. Radiocarbon AMS towards its low energy limits. Nucl Instrum Methods 223/224:339–345.

Synal HA, Stocker M, Suter M. 2007. MICADAS: A new compact radiocarbon AMS system. In proceedings of the 10th International Conference on Accelerator Mass Spectrometry, Berkeley, CA. Nucl Instrum Methods B 259:7–13.

Uhl T, Luppold W, Scharf A, Kritzler K, Kretschmer W. 2007. Development of an automatic gas handling system for microscale AMS ^{14}C measurements. In proceedings of the 10th International Conference on Accelerator Mass Spectrometry, Berkeley, CA. Nucl Instrum Methods B 259:303–307.

Valladas H, Clottes J, Geneste JM, Garcia MA, Arnold M, Cachier H, Tisnerát-Laborde N. 2001. Evolution of prehistoric cave art. Nature 413:479.

Valladas H. 2003. Direct radiocarbon dating of prehistoric cave paintings by accelerator mass spectrometry. Meas Sci Technol 14:1487–1492.

Wallner A, Arazi A, Faestermann T, Knie K, Korschinek G, Maier HJ, Nakamura N, Rühm W, Rugel G. 2004. ^{41}Ca—A possible neutron specific biomarker in tooth enamel. Nucl Instrum Methods B 223–224:759–764.

Vasil'chuk AC, Kim JC, Vasil'chuk YK. 2004. The AMS dating of pollen from syngenetic ice-wedge ice. Nucl Instrum Methods B 223/224:645–649.

Wiebert A, Persson P, Elfman M, Erlandsson B, Hellborg R, Kristiansson P, Stenström K, Skog G. 1996. Isobar suppression in accelerator mass spectrometry by the detection of characteristic X-rays. Nucl Instrum Methods B 109/110:175–178.

Vogel JS, Southon JR, Nelson DE, Brown TA. 1984. Performance of catalytically condensed carbon for use in accelerator mass spectrometry. Nucl Instrum Methods B 5(2):289–293.

Vogel JS. 1992. Rapid production of graphite without contamination for biomedical AMS. Radiocarbon 34(3):344–350.

Vogel JS. 2000. Accelerator mass spectrometry for human biochemistry: The practice and the potential. Nucl Instrum Methods B 172:884–891.

Yiou F, Raisbeck GM, Christensen CG, Holm E. 2002. ^{129}I/^{127}I, ^{129}I/^{137}Cs and ^{129}I/^{99}Tc in the Norwegian coastal current from 1980 to 1988. J Environ Radioactivity 60:61–71.

Yumoto S, Nagai H, Kobayashi K, Tada W, Horikawa T, Matsuzaki H. 2004. ^{26}Al incorporation into the tissues of suckling rats through maternal milk. Nucl Instrum Methods B 223/224:754–758.

Zhou WJ, Chen MB, Liu YH, Donahue D, Head J, Lu XF, Jull AJT, Deng L. 2000. Radiocarbon determinations using a minicyclotron: Applications in archaeology. Nucl Instrum Methods B 172:201–205.